Scanning-HIS: Vibration-induced tilt noise, tilt monitoring & correction algorithms

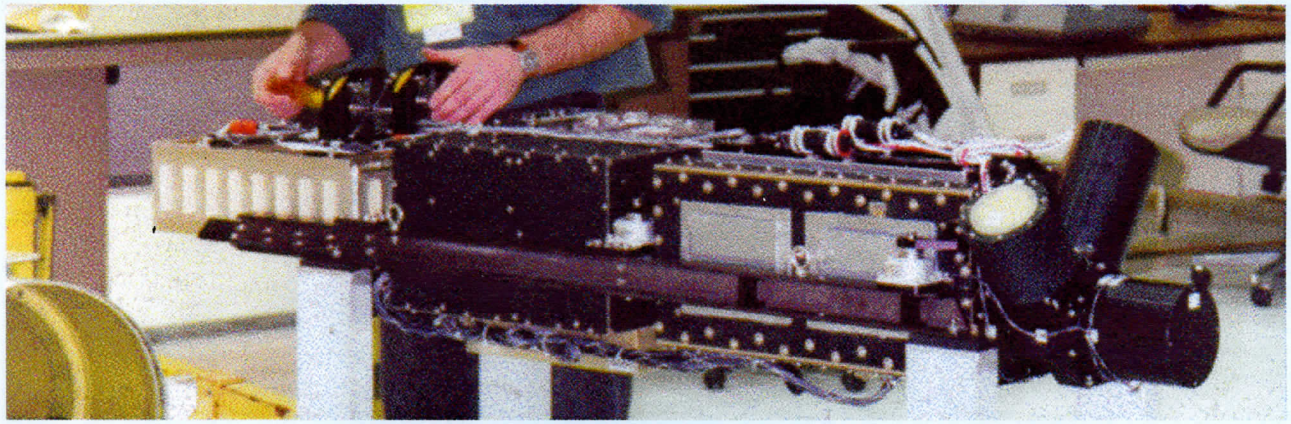

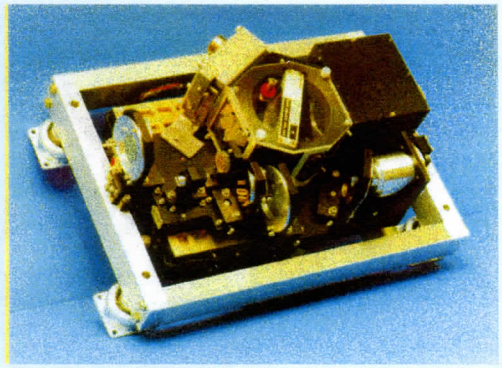

Hank Revercomb
University of Wisconsin, Space Science and Engineering Center

IPO SOAT Meeting, Silver Springs, MD, 15 March 2002

Topics

1. Scanning HIS Overview
2. Vibration-induced Tilt Noise: Amplitude Modulation
3. Vibration-induced Tilt Noise: Sample Position Errors
4. Tilt Issue Applicability to CrIS
5. PCA Random Noise Filtering Results

❶ Scanning HIS Overview

(HIS= High-resolution Interferometer Sounder)

Roots:
- U. of Wisconsin HIS Program, 1978-present
- 1st U2/ER2 HIS, 1985-present
- NAST-I, close cousin, for NPOESS testbed (Wingpod)
- S-HIS 1st Mission: CAMEX 3, 1998

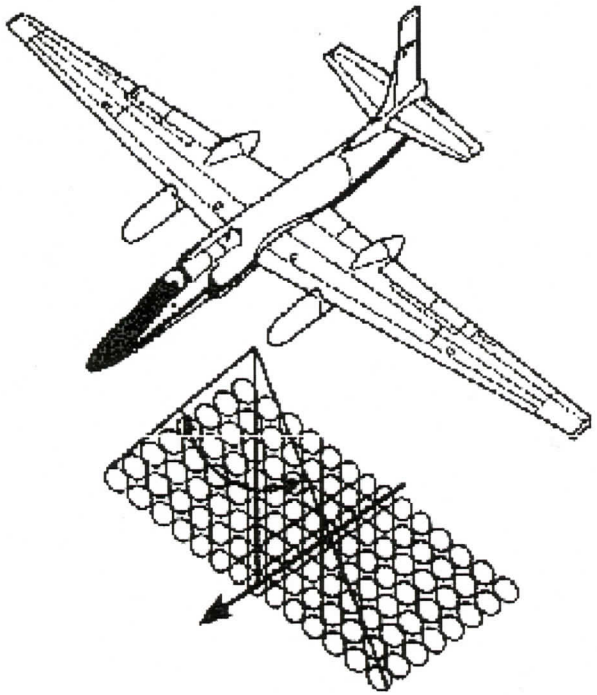

Characteristics:

Spectral Coverage:	3-17 microns
Spectral Resolution:	0.5 cm^{-1}
Resolving power:	1000-6000
Footprint Diameter:	100 mrad
Cross-Track pattern:	Programmable

(typically 15 pixels or Nadir only)

Scanning HIS Radiances-24 August 2000

SAFARI Terra Overpass-Clear Water

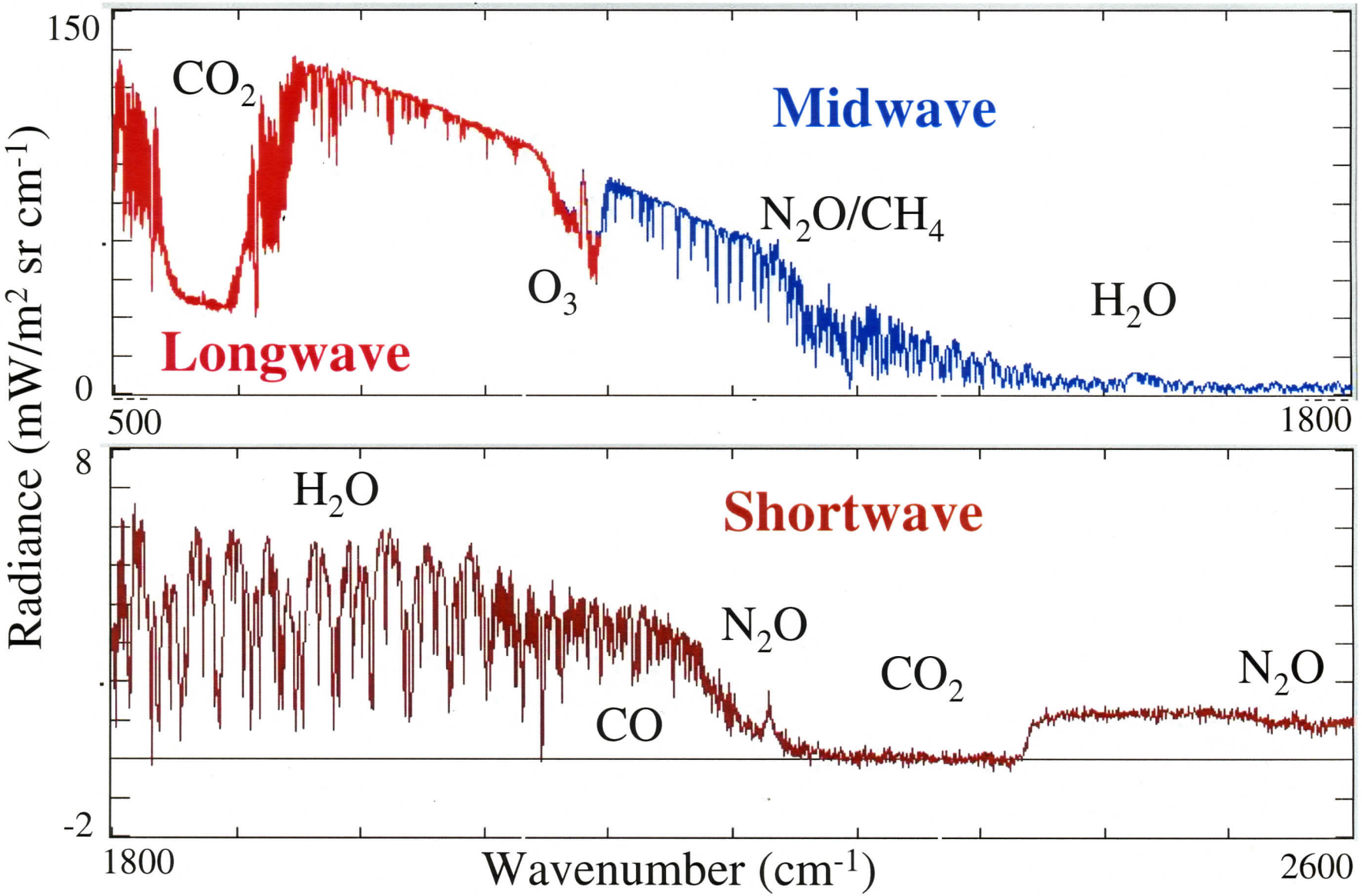

S-HIS Mission Summary

(1998-2000)

Experiment	Location	Time	Aircraft	# Flights/# Hours
CAMEX-3	Patrick AFB, Florida	September 1998	DC-8	6 / 36
WINTEX	Madison, Wisconsin	March 1999	ER-2	8 / 30
KWAJEX	Kwajalein Atoll	Aug-Sept 1999	DC-8	35 / 172
WISC-T2000	Madison, Wisconsin	March 2000	ER-2	8 / 30
SAFARI	Pietersburg, South Africa	Aug-Sept 2000	ER-2	15 / 80
AFWEX	ARM CF, Oklahoma	Nov-Dec 2000	DC-8	8 / 50
		TOTAL	DC-8	258 hours
			ER-2	140 hours

Okavanga Delta Mapping

from Scanning HIS, SAFARI, 27 Aug 2000

Scanning HIS: 2 km footprints

T_b (980-985 cm^{-1})

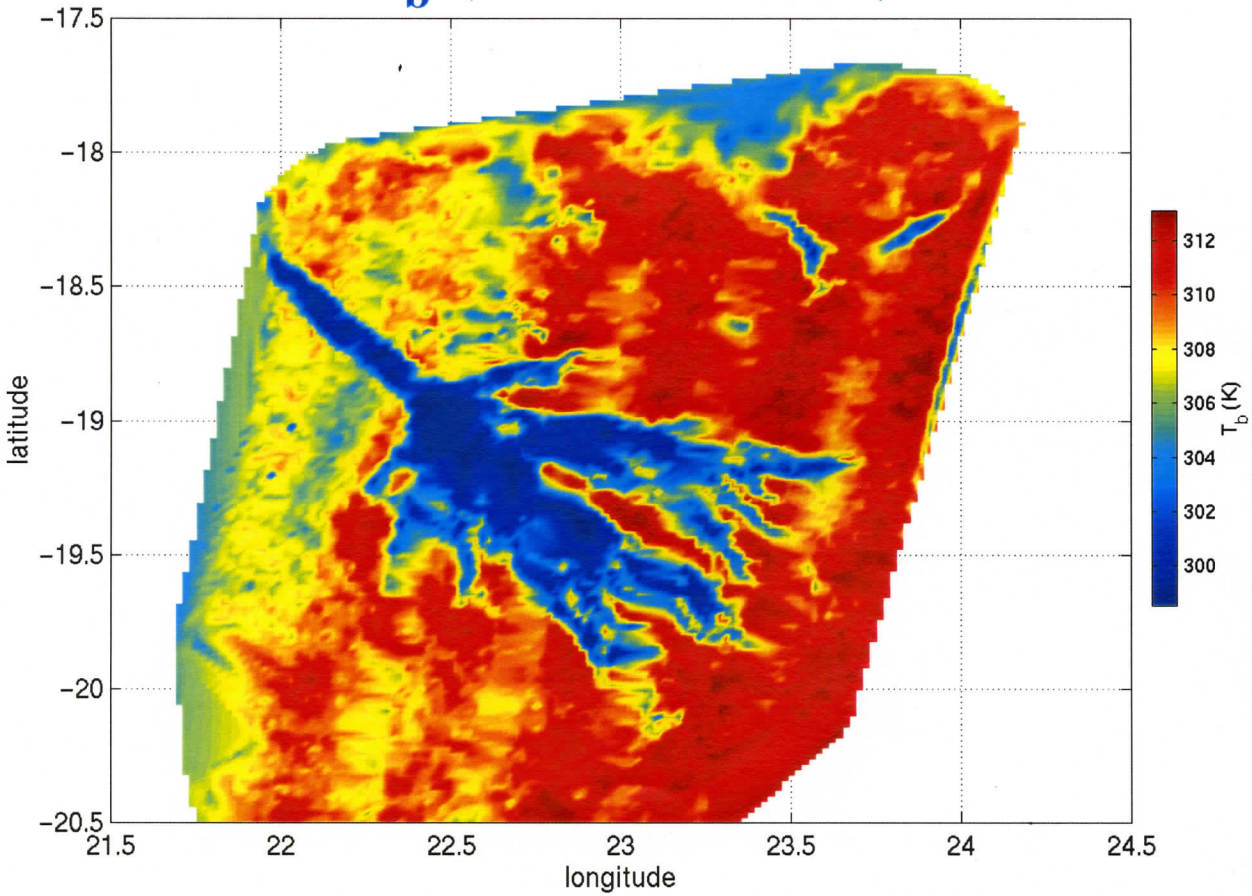

MODIS: 0.25 km

0.65 μm

Surface Emissivity, a new emphasis

Namibian Land (11 September 2000)

Brightness T

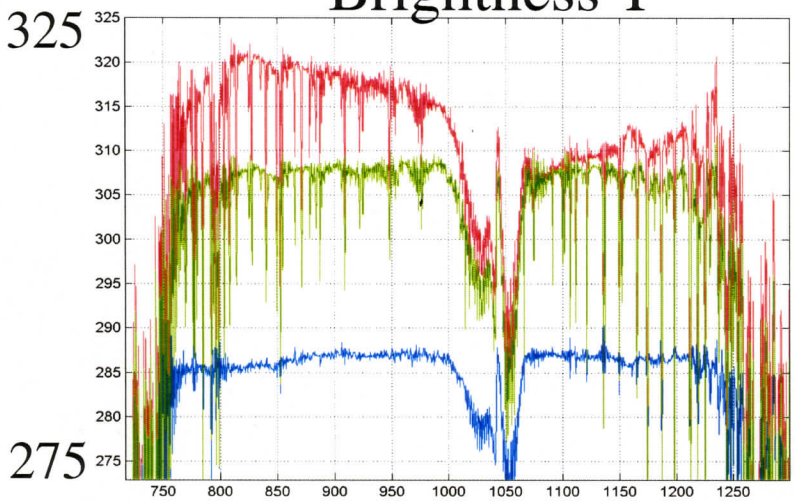

Emissivity

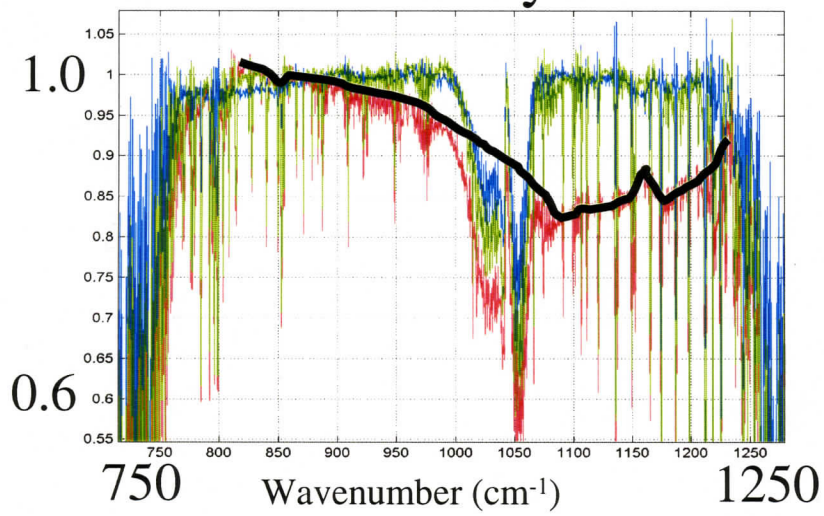

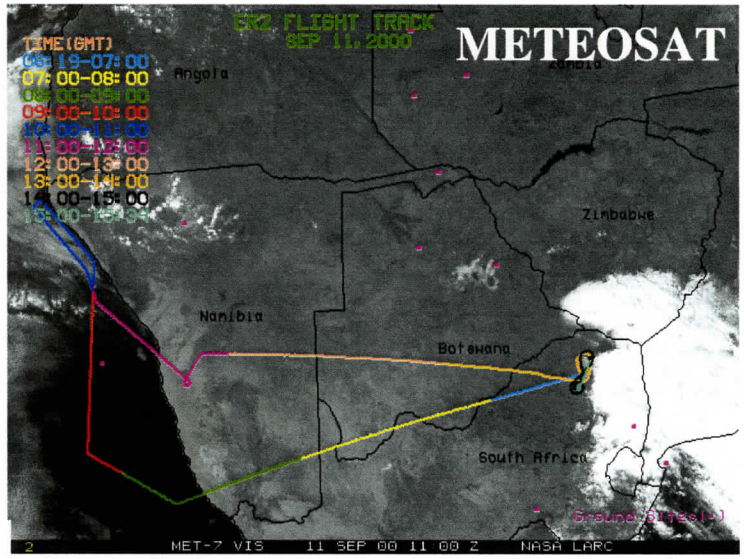

Namibian Coast

- Kuiseb River Canyon
- [Dunes (left)≈Desert pavement]
- Kalahari Desert (Vegetated)
- Ocean

Burn Scar Surface Characteristics

(7 September Controlled Burn)

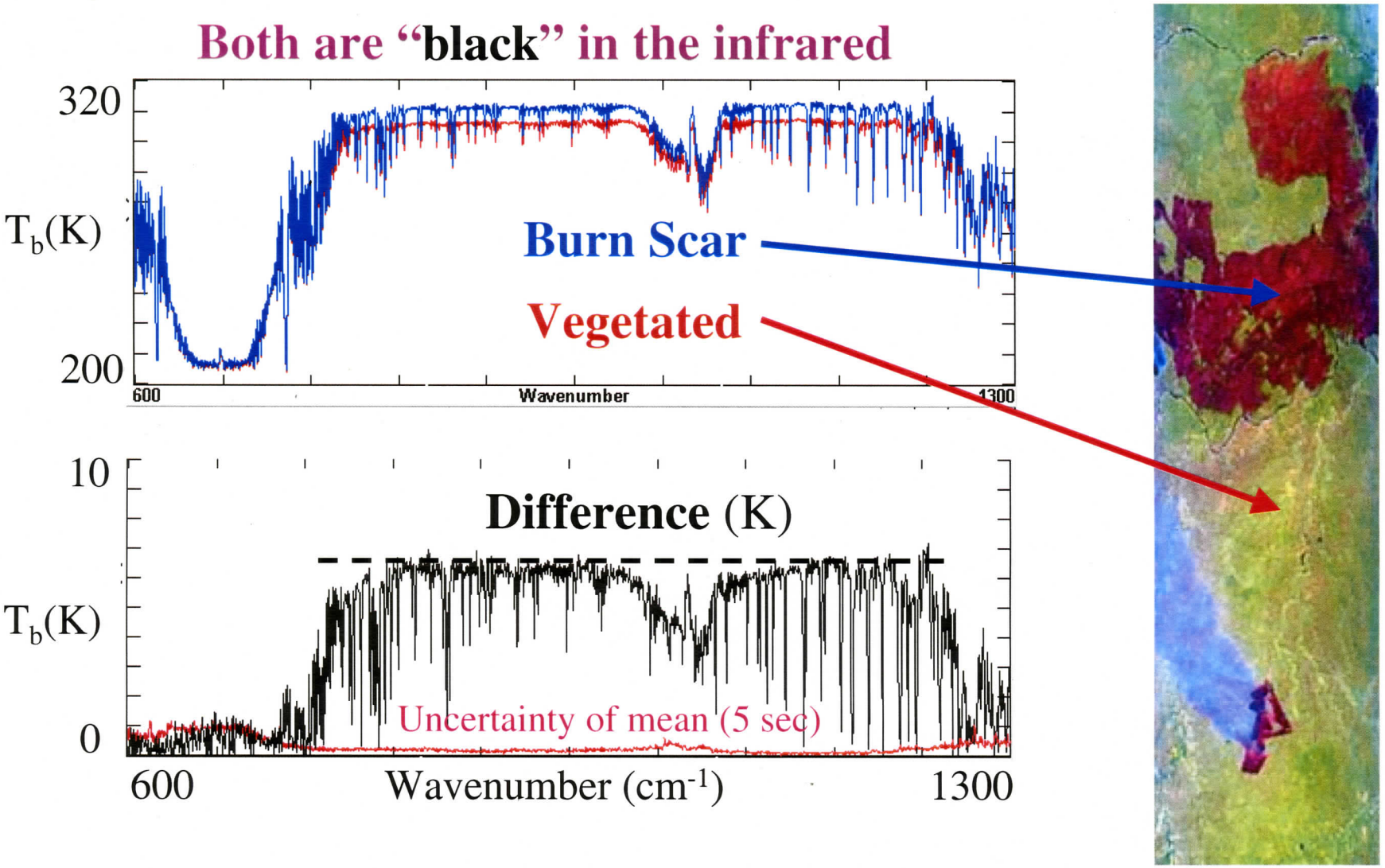

Fire Radiometric Signature

(1 Sept Night Flight, 7 Sept Controlled Burn)

- High temperature and enhanced CO_2 provide a unique "**blue Spike**" signature in high resolution spectra

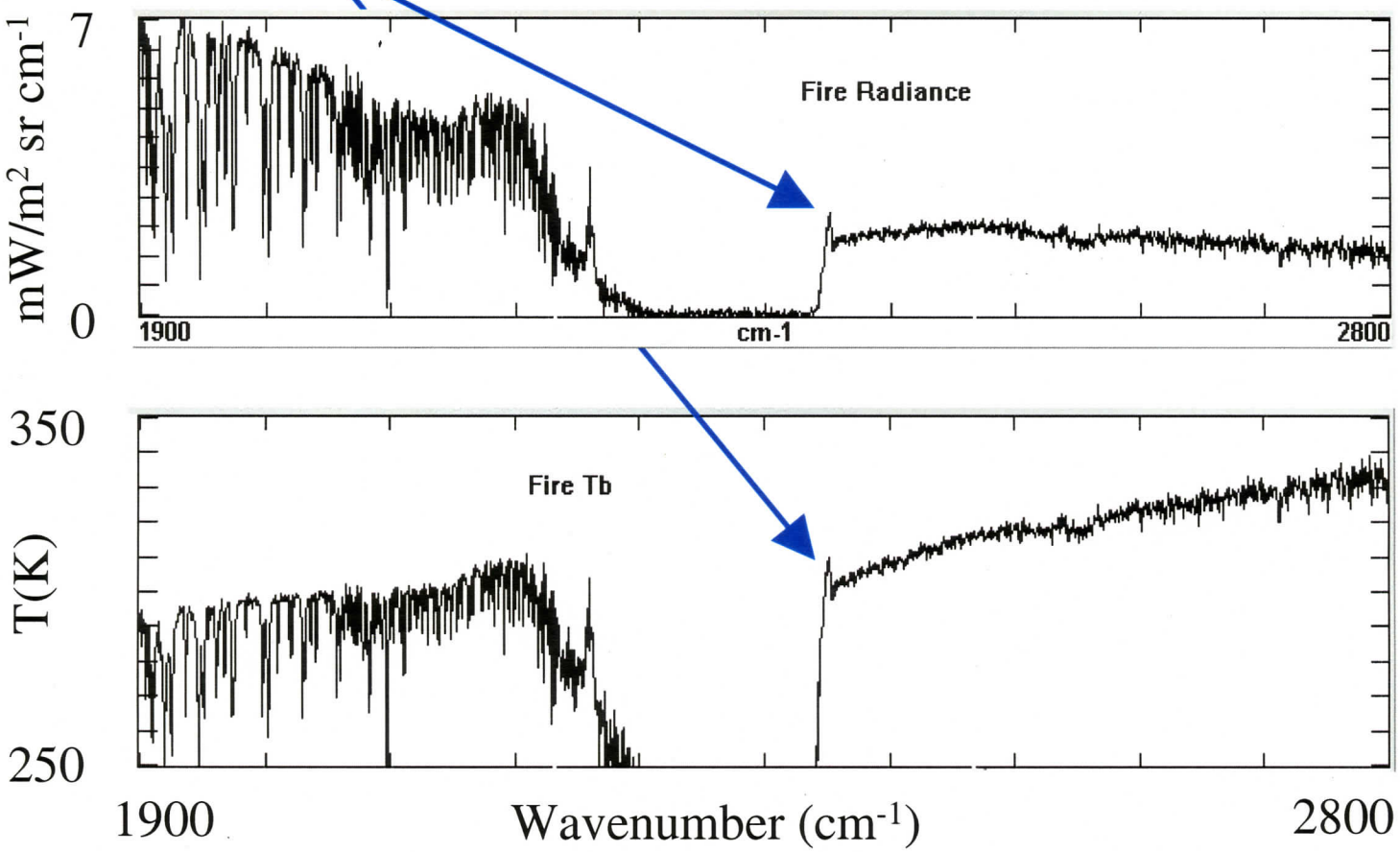

MAS

CO Detection over Fire
(1 Sept Night Flight)

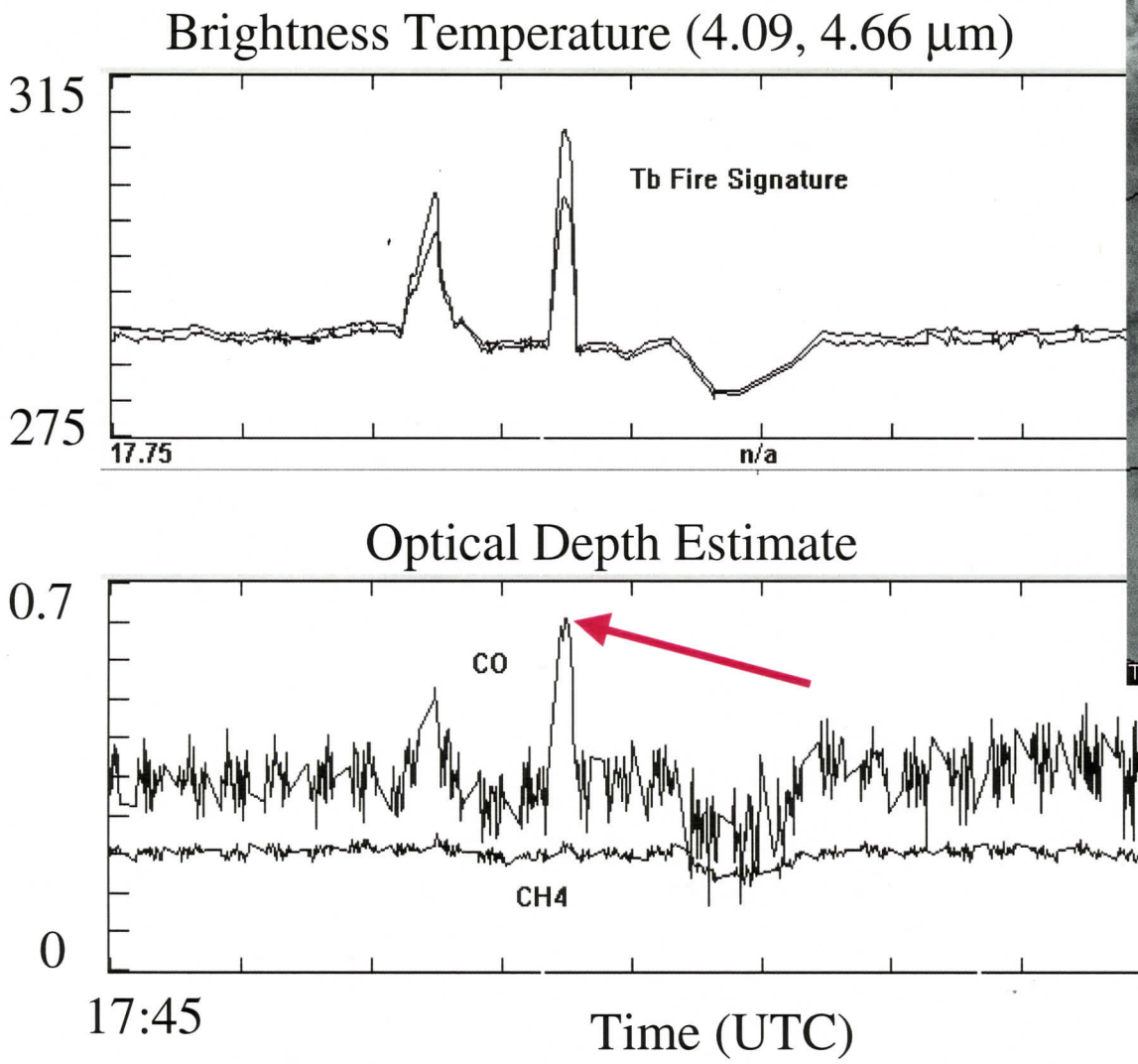

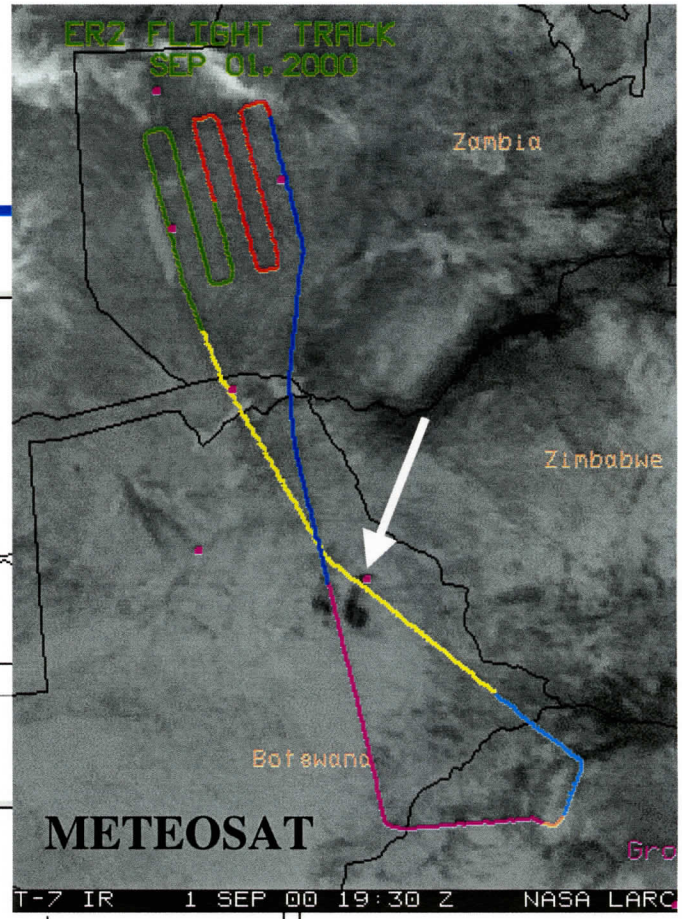

Column CO doubles over the fire

WVIOP 2000 and AFWEX

Southern Great Plains ARM Site Water Vapor Experiments

WVIOP 2000: 18 Sept - 8 Oct 2000. **Goal**: 2% pwv

AFWEX: 27 Nov - 15 Dec 2000. **Goal**: 10% of uppermost 0.1mm

Sensors: Microwave Radiometers, Vaisala and VIZ radiosondes, chilled mirror sondes, ground and tower based in-situ sensors, Raman Lidar, ground and ac-based DIAL, GPS, solar, AERI, SHIS, NASTI, GOES, aircraft based frost point hygrometer, tunable diode laser hygrometer

Current Perspective:

- MWR, tower scaled Raman Lidar, and nighttime corrected sondes agreeing to ~3 % in pwv. GPS, Solar, raw sondes all drier by 3-10 %.
- Sondes are ~20% drier than Raman Lidar at 8-12km, but upper level "truths" (in-situ) agreeing better with sondes than with Raman Lidar.

Scanning-HIS Spectra from AFWEX level legs

7.5-12.5 km, 5 Dec 2000

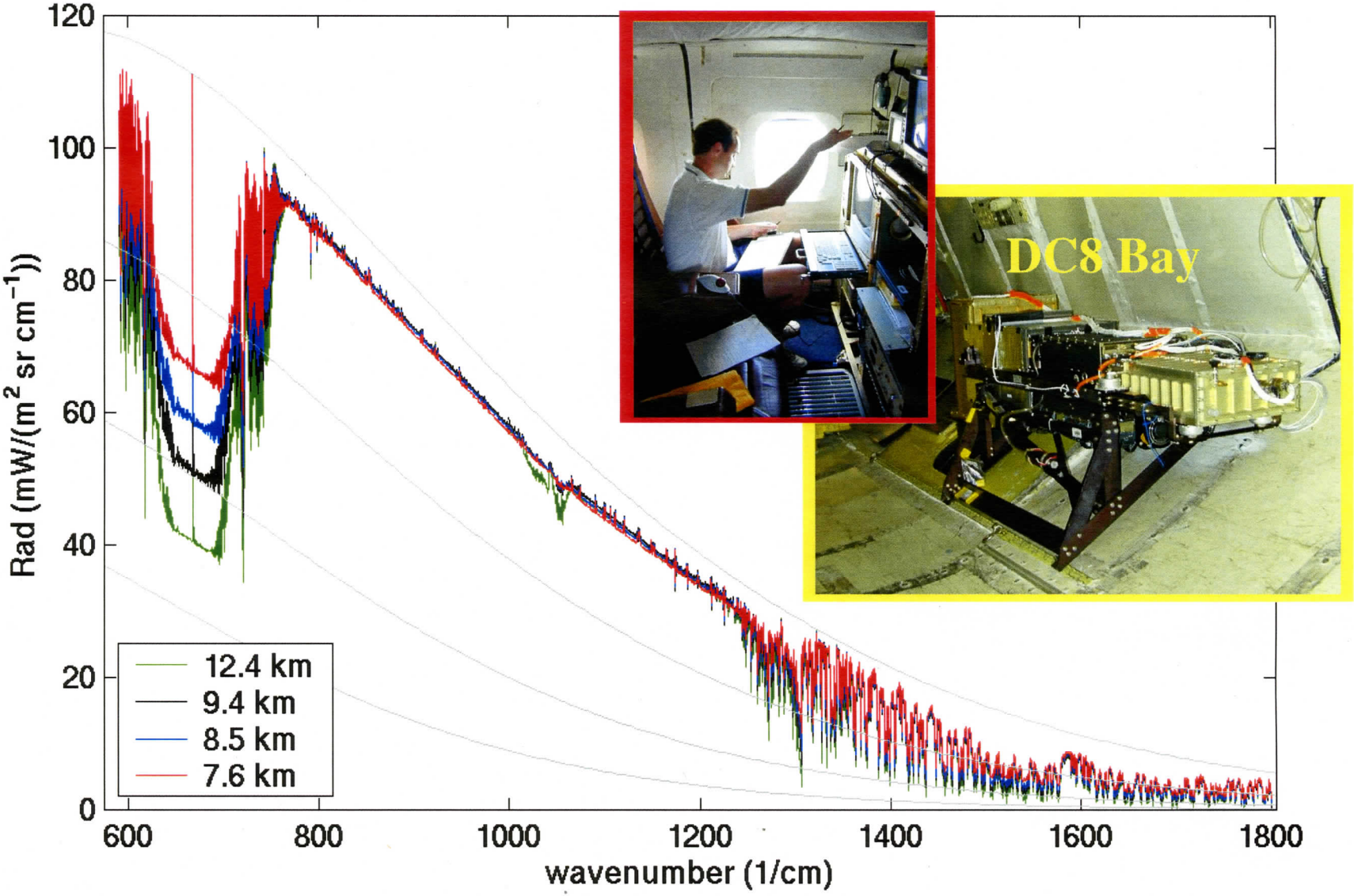

Calculation from Sonde Compared to S-HIS Brightness T Spectra

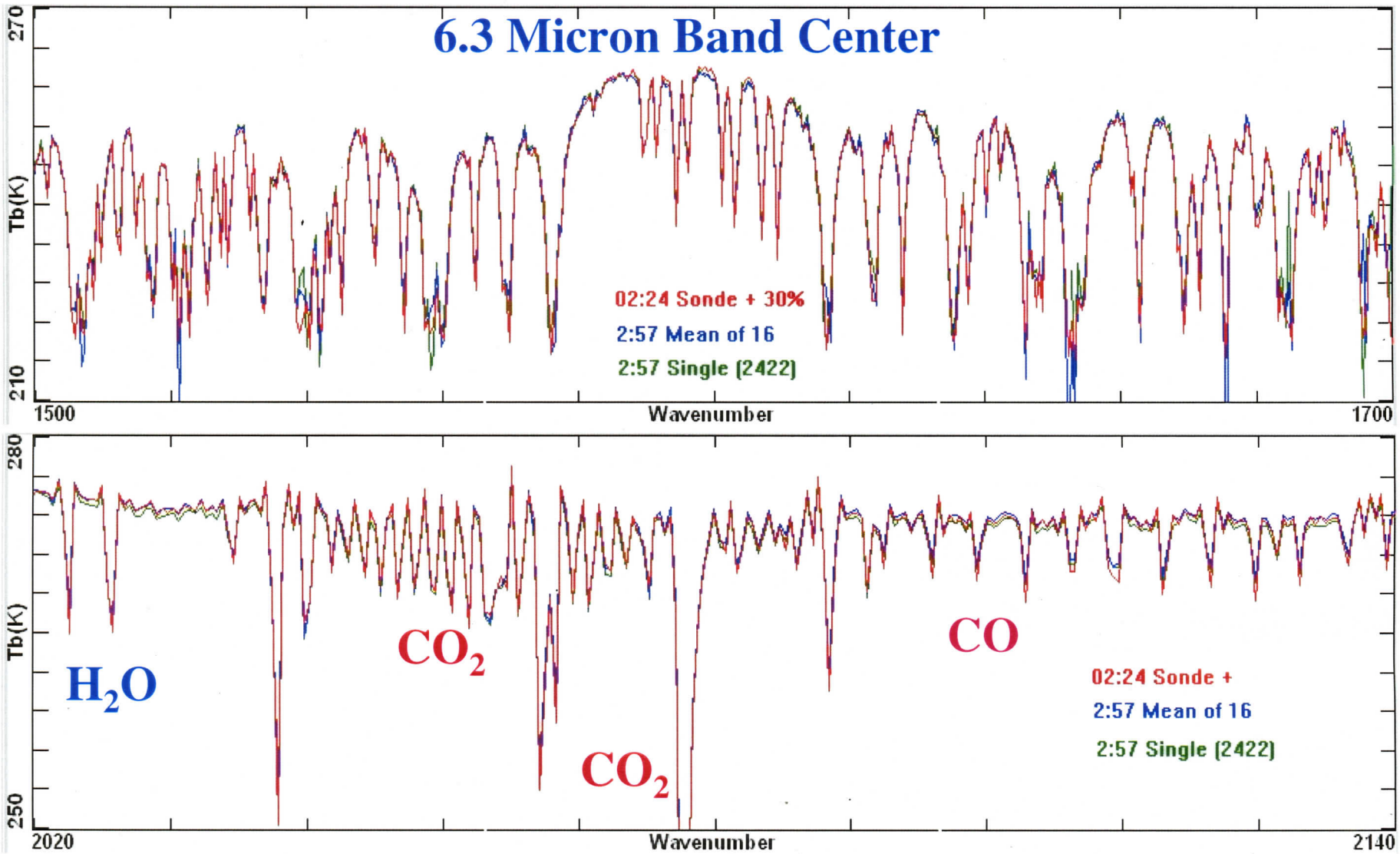

12-10-00 AFWEX

S-HIS Mission Summary

(2001-2002)

Experiment	Location	Time	Aircraft
Texas-2001	San Antonio, Texas	March 2001	ER-2
CLAMS	Wallops Island Virginia	July 2001	ER-2
IHOP	Oklahoma	May-June 2002	DC-8
Grand Tour ARM SGP	Oklahoma	October 2002	Proteus
Aqua Val	Texas	Fall 2002/ Early 2003	ER-2
Grand Tour ARM NSA	Alaska	April-May 2003	Proteus

NASTI & Scanning HIS Comparisons at CLAMS, 17 July 2001

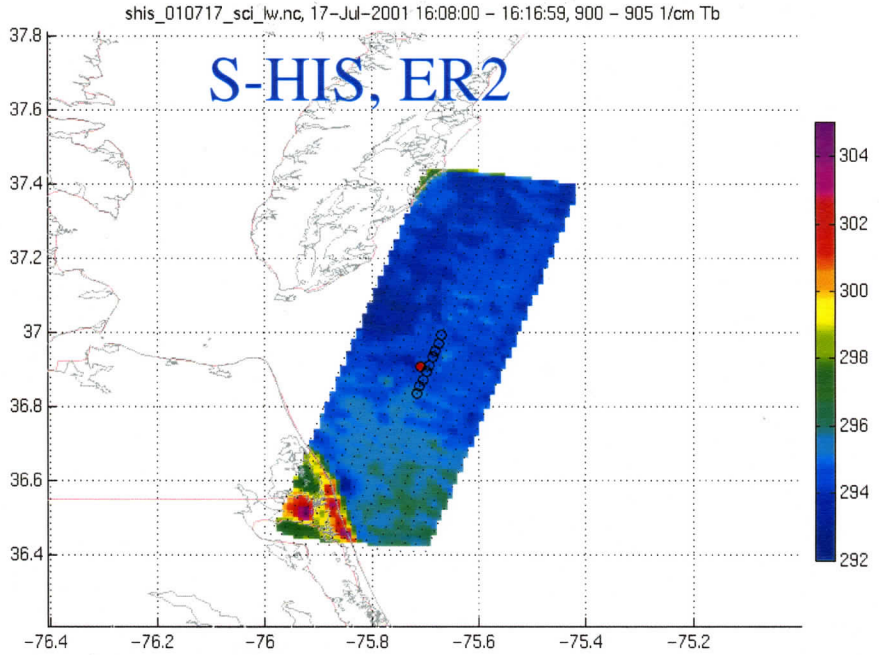

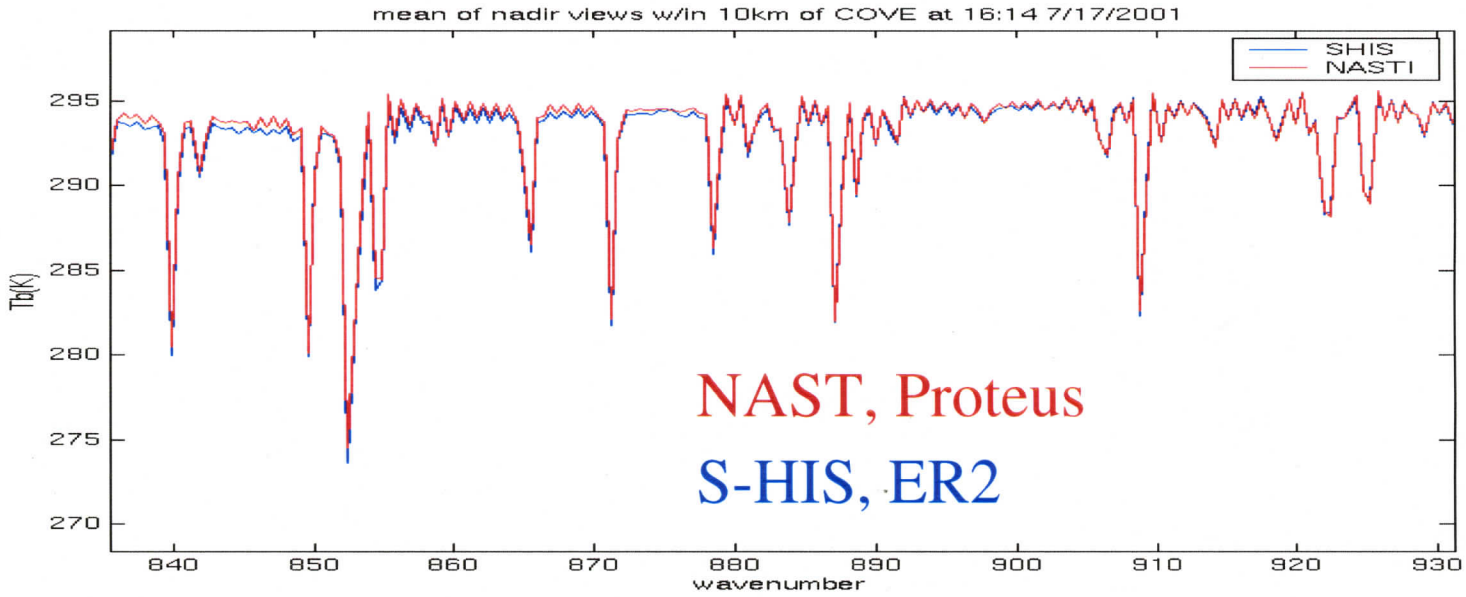

Proteus Installation Under Design for ARM

- NPOESS Atmospheric Sounder Testbed Interferometer (NAST-I) Microwave (NAST-M)
- Far-Infrared Sensor for Cirrus (FIRSC)

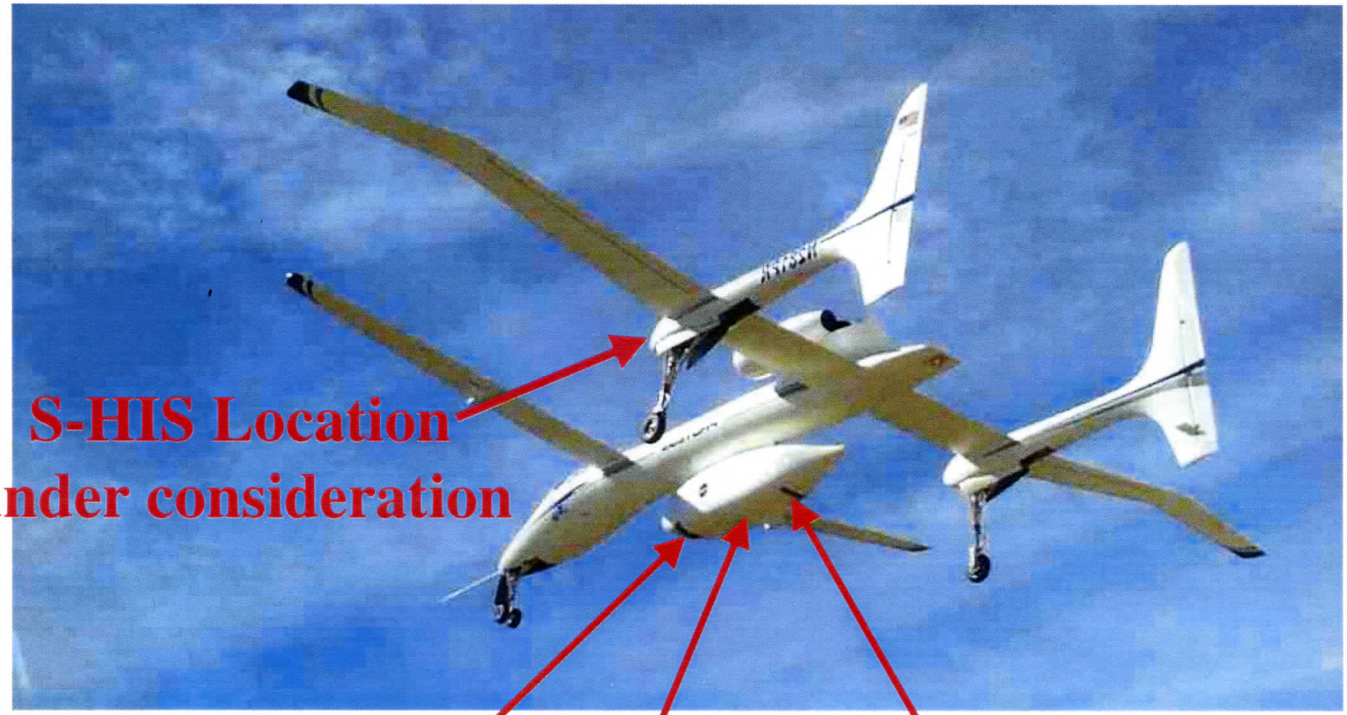

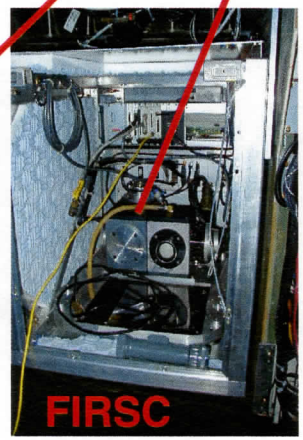

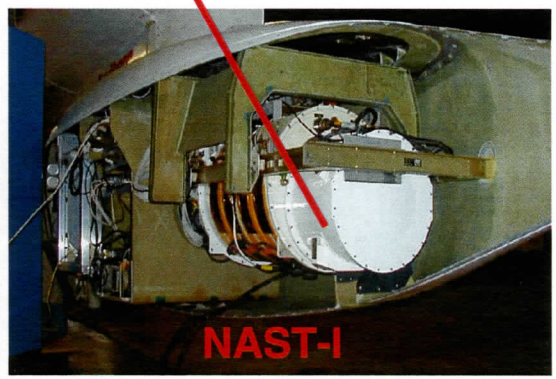

❷ Vibration-induced Tilt Noise: Amplitude Modulation

- Definition of effect
- Nature of Tilts & Verification of effect on IR Spectra
- Correction Relationships

UW Vibration-Induced Tilt Study Events

(largely under IPO support)

- 1996: S-HIS aperture sharing concept: Henry Buijs alerted us to the sample position error risk & initial theory defined
- 1998: Participation in NAST tilt noise characterization
- 12/1998: 1st tilt monitoring using housekeeping system on S-HIS
- 1999: Current tilt monitoring board installed on S-HIS (June) & UW tilt correction algorithms defined
- 2000: Concept of both magnitude and sample-position tilt errors and tilt measurement system verified with real data
- 6/2000: New OPD drive mechanism developed and implemented on S-HIS to reduce tilts
- 6/2001: S-HIS & NAST Dynamic alignment electronics modified to allow compensation for optical static tilts
- 6/2001: S-HIS dynamic alignment mechanism modified to damp system resonance
- 2000-02: Correction software efforts (intermittent)

Tilts Reduce Spectral Amplitudes

- Wavefront Tilts θ_t reduce spectral amplitudes by factors:

$$2\,J_1(z)/z \cong [1 - z^2/8 + z^4/192 - \ldots], \text{ circular beam} \quad (1)$$

$$\sin(z)/z \cong [1 - z^2/6 + z^4/120 - \ldots], \text{ square beam} \quad (2)$$

where J_1 is a first order Bessel function, $z = 2\pi\,\nu\,R\,\theta_t$, R is the radius (or ½ side of the square) of the beam, & ν is the wavenumber. Note: effect $\propto$ wavenumber^2 & R^2 making it much larger for SW band on S-HIS

- $$\theta_t^2(x,\nu) = [\theta_{x0}(\nu) + \theta_x(x)]^2 + [\theta_{y0}(\nu) + \theta_y(x)]^2$$
$$= [\theta_{x0}^2(\nu) + \theta_{y0}^2(\nu)] + [\theta_x^2(x) + \theta_y^2(x)]$$
$$+ 2\,[\theta_{x0}(\nu)\,\theta_x(x) + \theta_{y0}(\nu)\,\theta_y(x)] \quad (3)$$

where the subscript 0 labels the ν-dependent static tilts

Effect of Tilts on Interferogram Amplitudes

- The result on an interferogram, for a circular beam to 1st order is

$$F(x) = \int d\nu \{1 - \tfrac{1}{2}[\pi \nu R \theta_t(x, \nu)]^2\} C_c \exp(i2\pi\nu x) \qquad (4)$$

where C_c is the correct complex spectrum (numerical filtering removed) that would result without tilt errors

- Separation of delay and wavenumber dependences allows rigorous expression as Fourier transforms

$$-\tfrac{1}{2}[\pi \nu R \theta_t(x, \nu)]^2 = -\tfrac{1}{2} (\pi R)^2 \sum G_i(\nu) H_i(x), \text{ where} \qquad (5)$$

$$G_1 = \nu^2 [\theta_{x0}^2(\nu) + \theta_{y0}^2(\nu)] \qquad H_1 = 1$$

$$G_2 = \nu^2 \qquad H_2 = [\theta_x^2(x) + \theta_y^2(x)]$$

$$G_3 = 2\nu^2\theta_{x0}(\nu) \qquad H_3 = \theta_x(x)$$

$$G_4 = 2\nu^2\theta_{y0}(\nu) \qquad H_4 = \theta_y(x)$$

S-HIS Dynamic Tilt Characteristics:

27 February 2000, WISC-T2000 on ER2

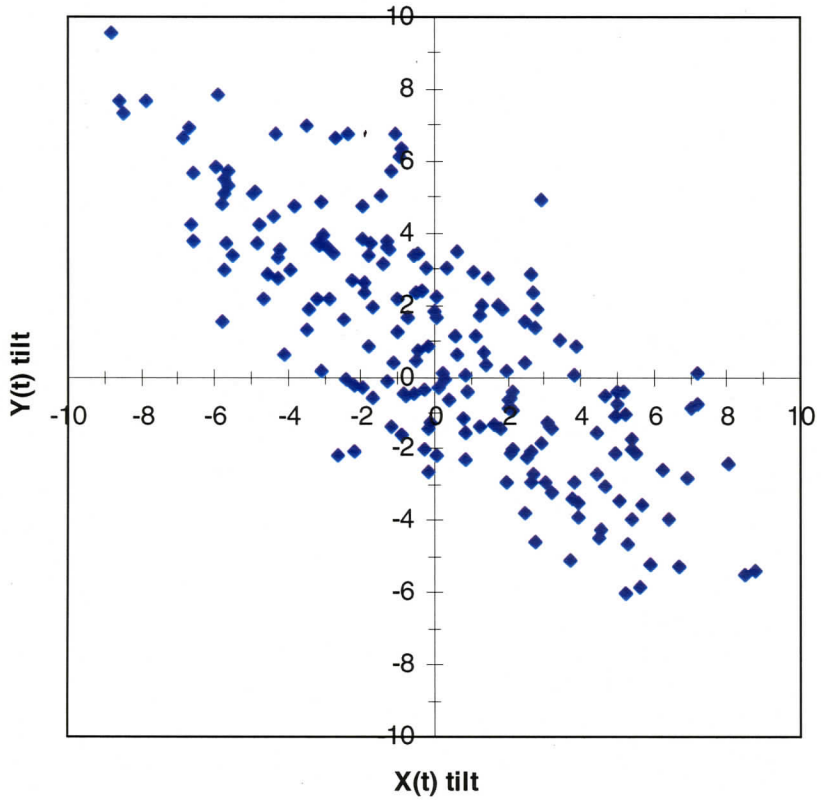

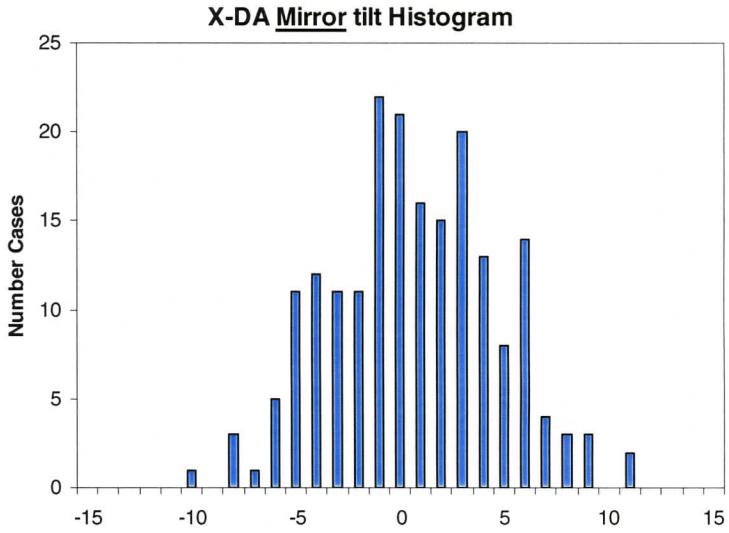

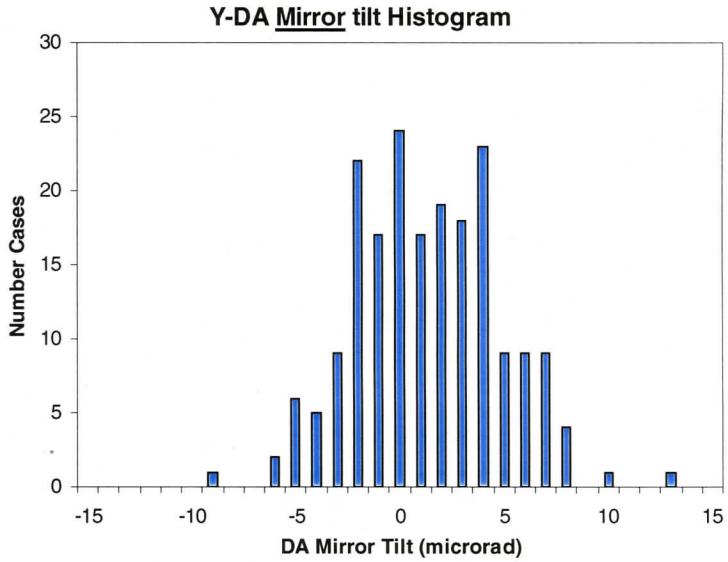

x & y Tilts measured every 8 laser fringes, 0-20 K Hz frequency band

S-HIS New Drive Reduced Tilts by factors of 2-5 from tilts discussed here

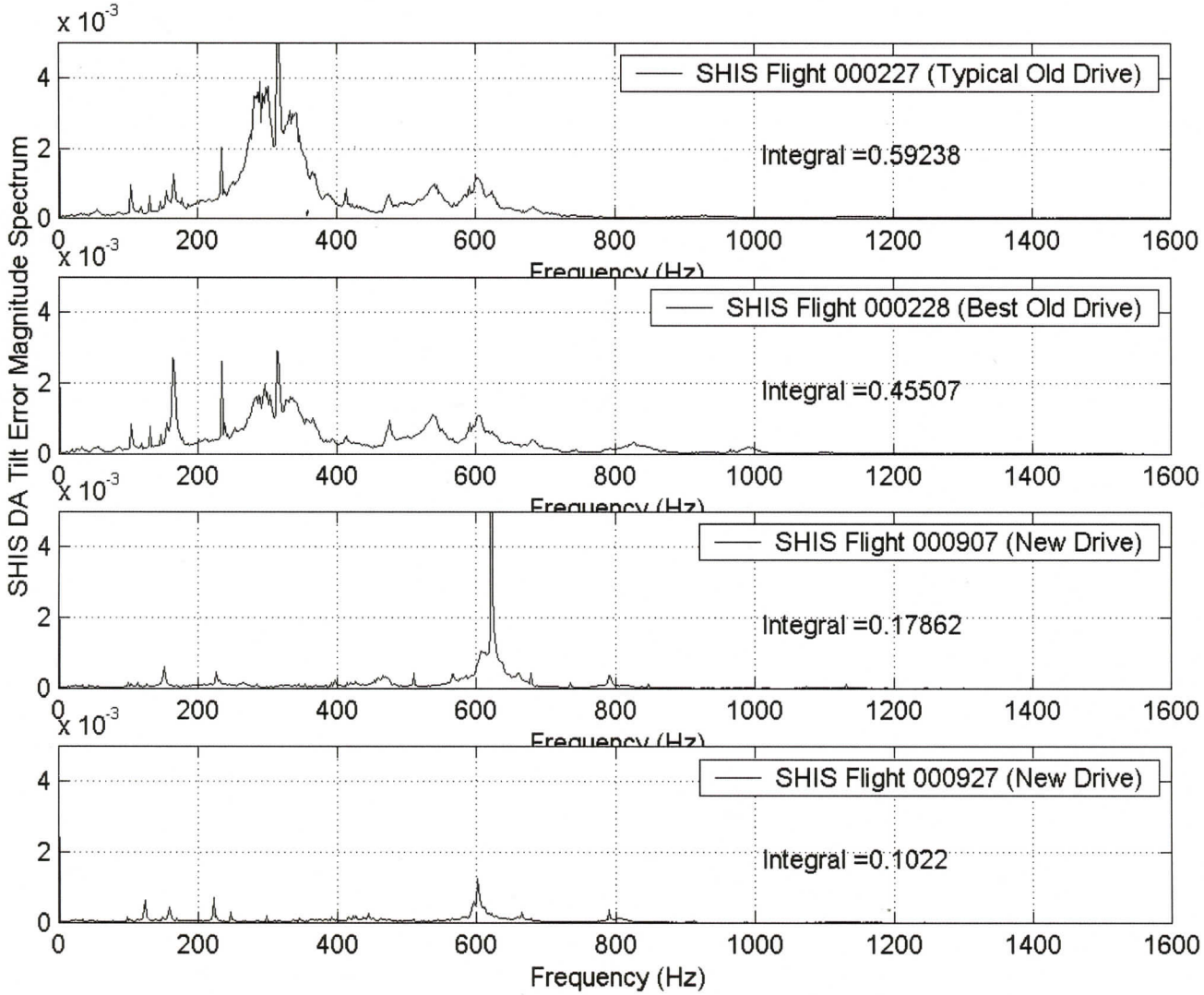

Tilt frequency distribution -

New drive removed major "300 Hz" resonance

S-HIS Shortwave Tilt Modulation:

27 February 2000, WISC-T2000 on ER2

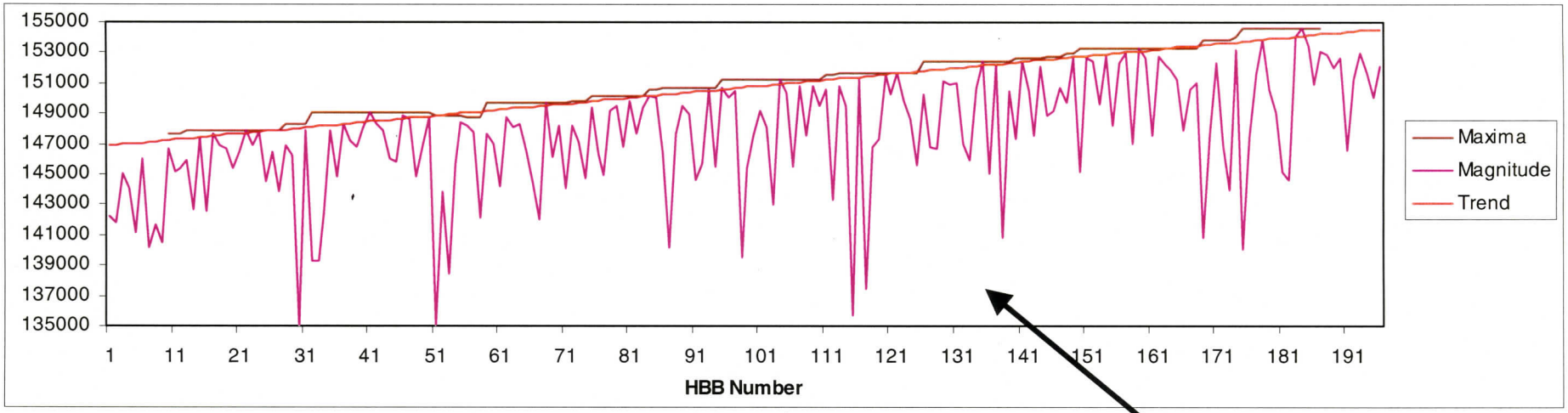

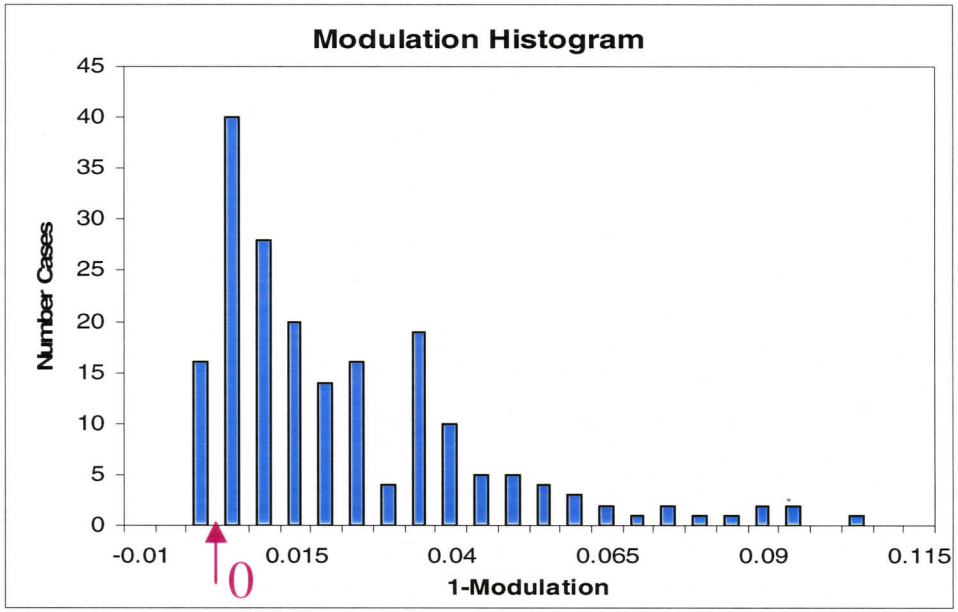

Average of HBB magnitude spectrum represents ZPD for consecutive HBB views

Tilt-Model Fit to Shortwave Modulation:

27 February 2000, WISC-T2000, ER2

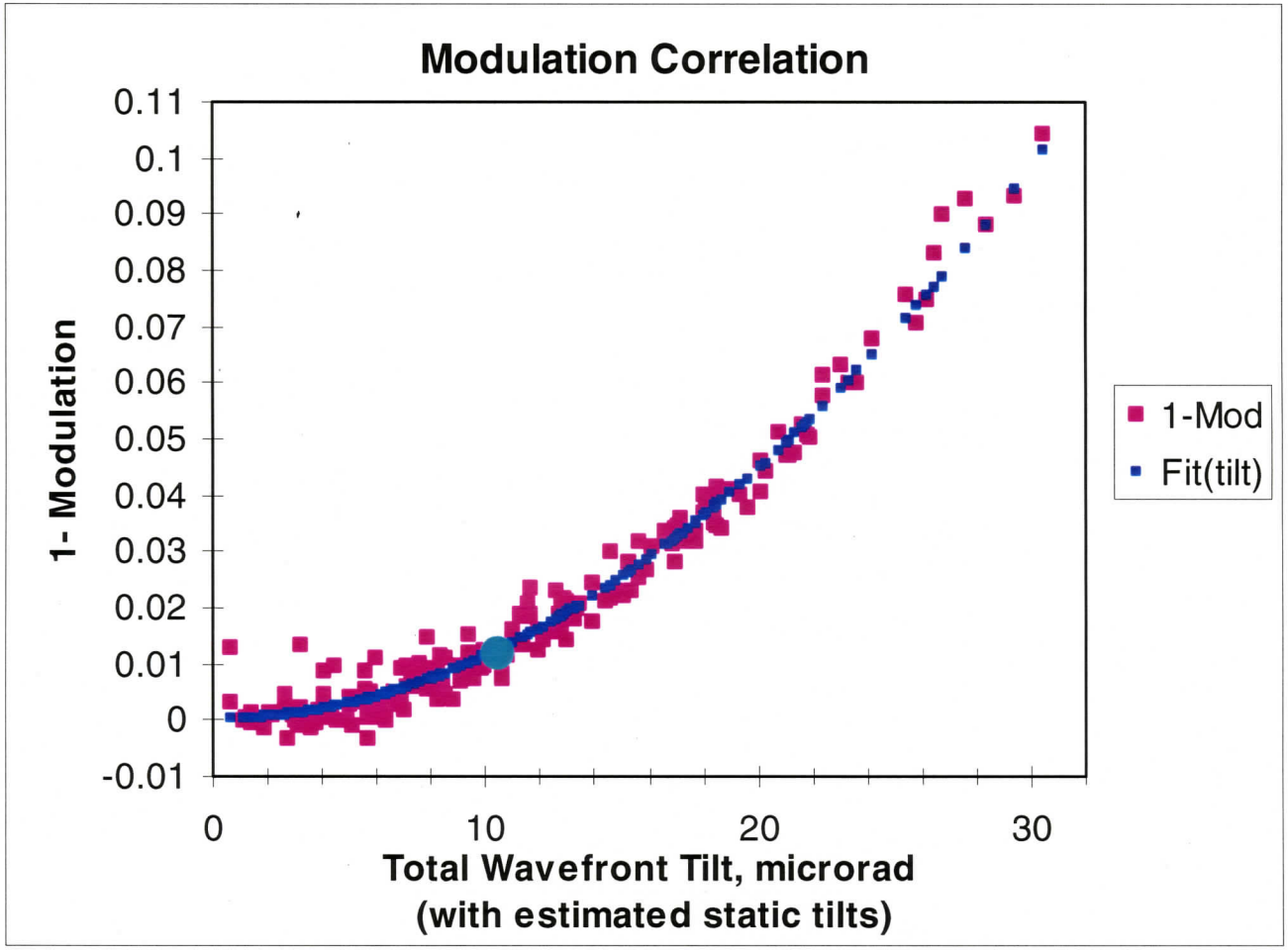

Static Tilt*

x= +6.3

y= -8.2 μrad

(adjusted to fit)

* (Electrically moved to near zero since this time)

Verifies tilt measurements and concepts

Tilt-Model Fit to Shortwave Modulation:

27 February 2000, WISC-T2000

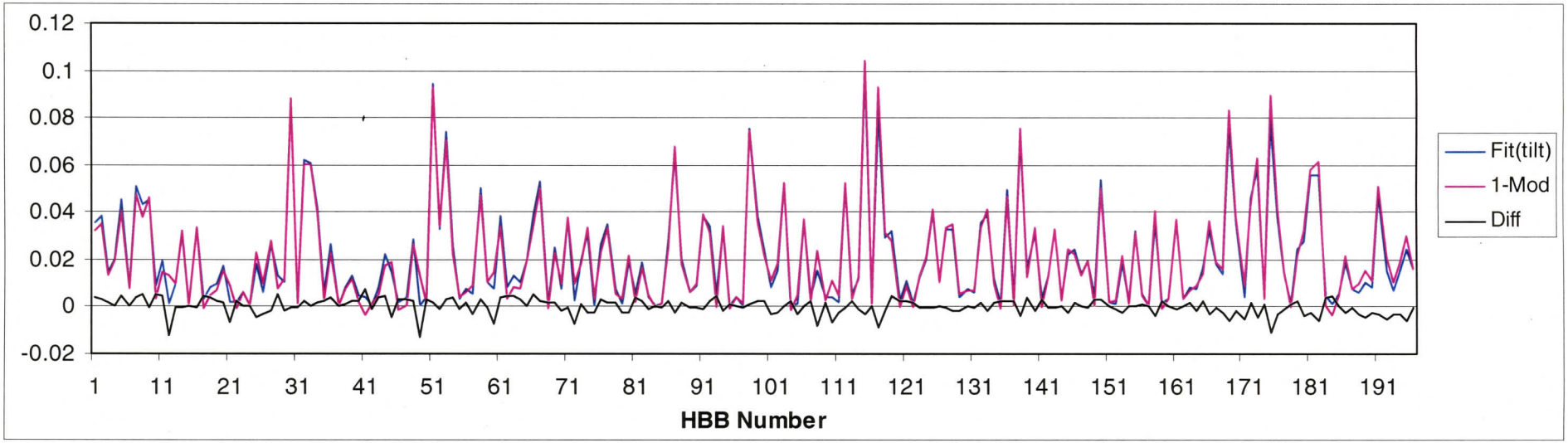

Static Tilt*

x= +6.3

y= -8.2 μrad

*(before electrical offset modification)

Correction for removing the effect of tilts on Interferogram Amplitudes

- $F(x) = \int d\nu\ C_c \exp(i2\pi\nu x)$

$$- \tfrac{1}{2}(\pi R)^2 \sum [H_i(x) \int d\nu\ G_i(\nu)\ C_c \exp(i2\pi\nu x)$$

$$= \mathbf{FT}\ (C_c) - \tfrac{1}{2}\ (\pi R)^2 \sum [H_i(x)\ \mathbf{FT}\ (G_i(\nu)\ C_c)] \qquad (6)$$

where Fourier transformation is indicated by "**FT**"

- The Corrected Spectrum resulting from **FT** of (6) is given by

$$C_c = C_0 + \tfrac{1}{2}(\pi R)^2 \sum \mathbf{FT}\ [H_i(x)\ \mathbf{FT}\ (G_i(\nu)\ C_c)] \qquad (7)$$

$$C_c \cong C_0 + \tfrac{1}{2}(\pi R)^2 \sum \mathbf{FT}\ [H_i(x)\ \mathbf{FT}\ (G_i(\nu)\ C_0)] \qquad (8)$$

Corrected SW Hot Blackbody Views Compared to Uncorrected

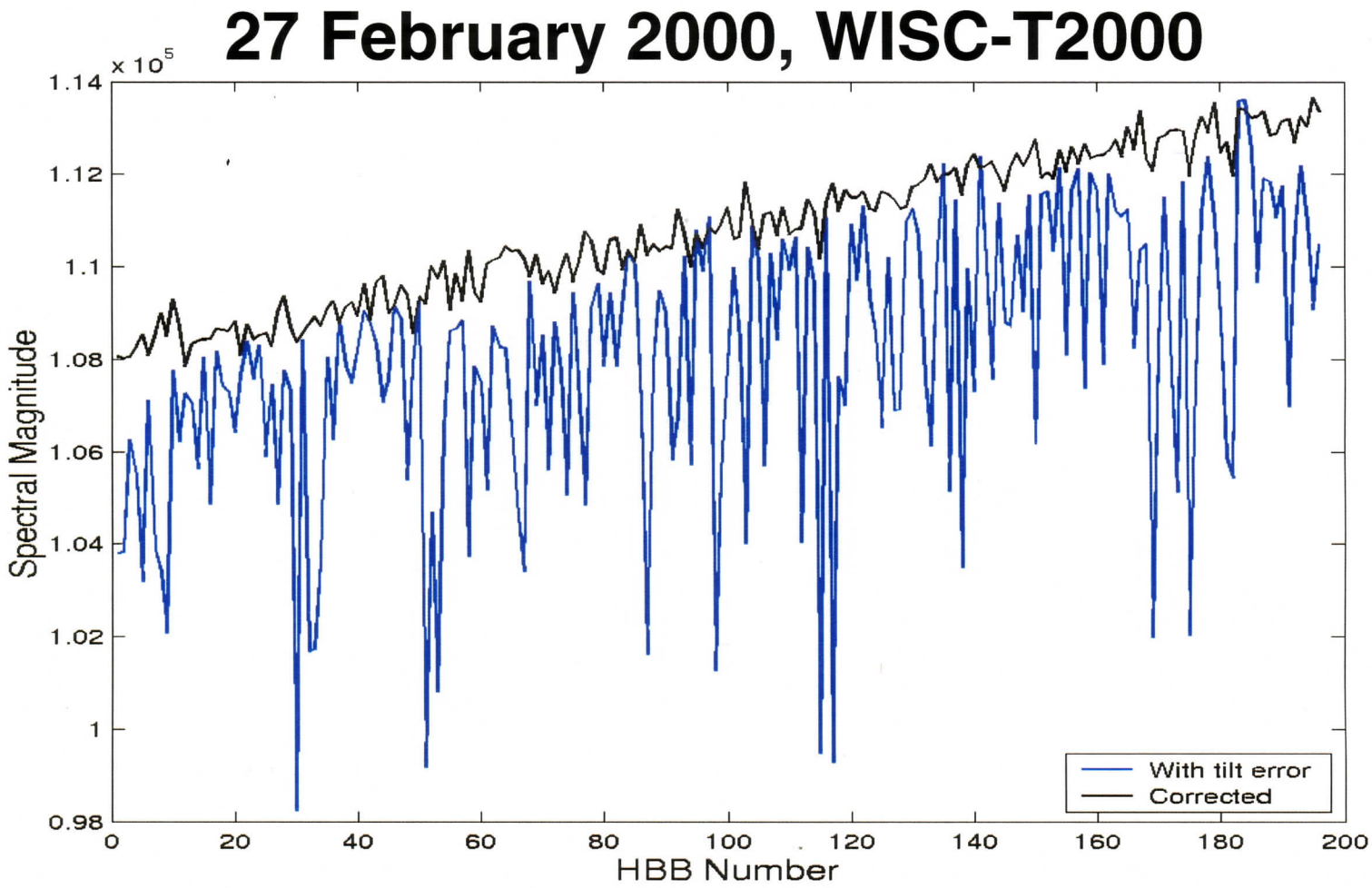

❸ Vibration-induced Tilt Noise: Sample Position Errors

- Definition of effect
- Verification of effect on IR Spectra
- Correction Relationships

Tilts cause OPD errors on S-HIS

- Tilt causes the OPD for each sample to differ from the uniformly-spaced sample positions triggered by laser signal zero crossings, because the center of the IR beams in the interferometer for the longwave (LW) and midwave (MW) bands are displaced from the location of the laser beam feeding the sample-triggering detector (by d ≈1 cm)

- The error is just $\delta x = \theta_d(x)\, d$ (1)

  where $\theta_d(x)$ is the component of the jitter tilt (not the total tilt including static tilt) in the direction from the sample-triggering beam center to the IR beam center (angle γ from x-axis)

- For S-HIS, these sample position errors dominantly cause low-resolution spectral rocking (not ghost lines). Phase variations result near ZPD (where tilts approximate a translation of F(x))

Scanning HIS Optical Configuration

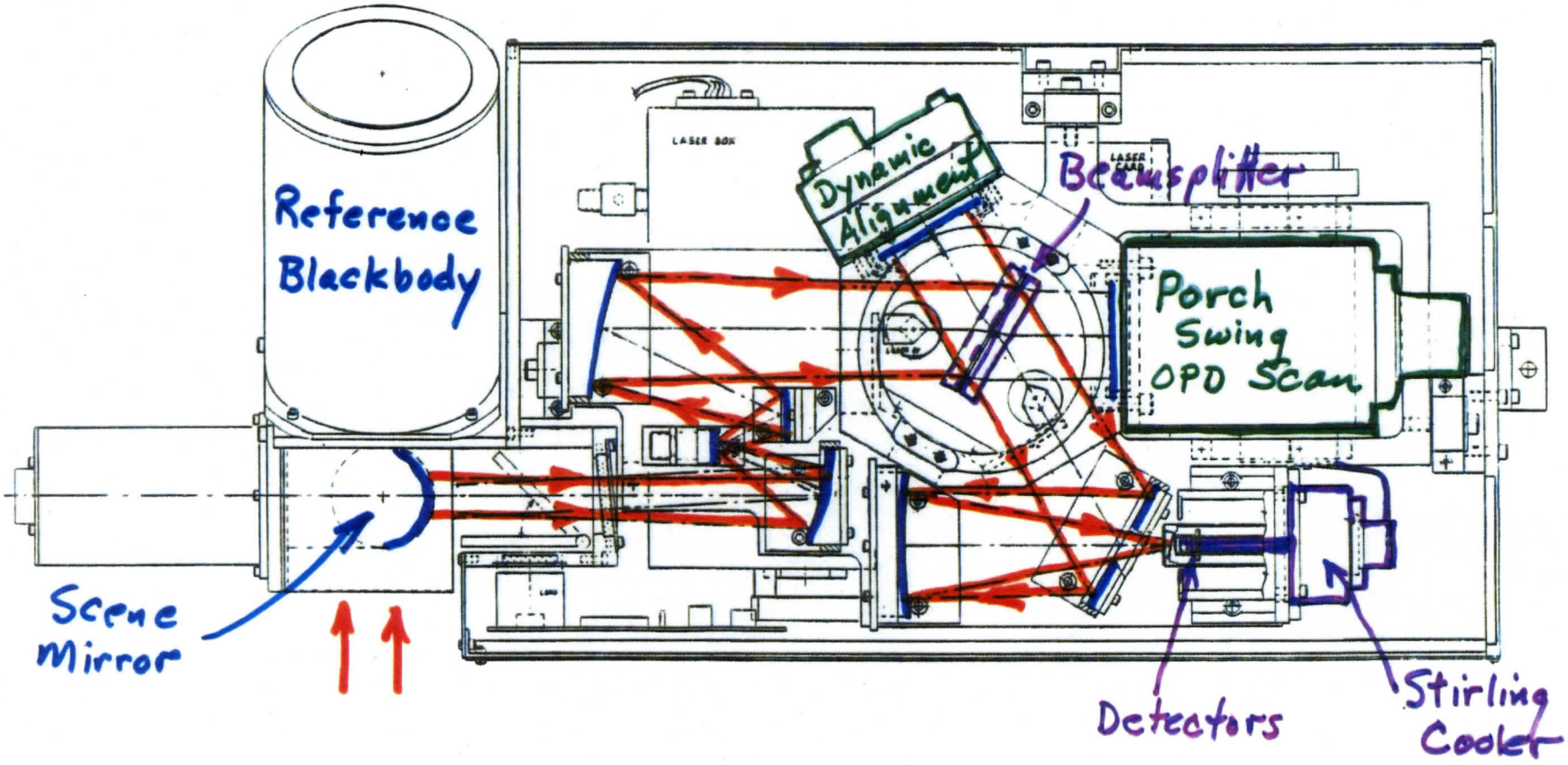

Scanning HIS Detector/Dewar Configuration

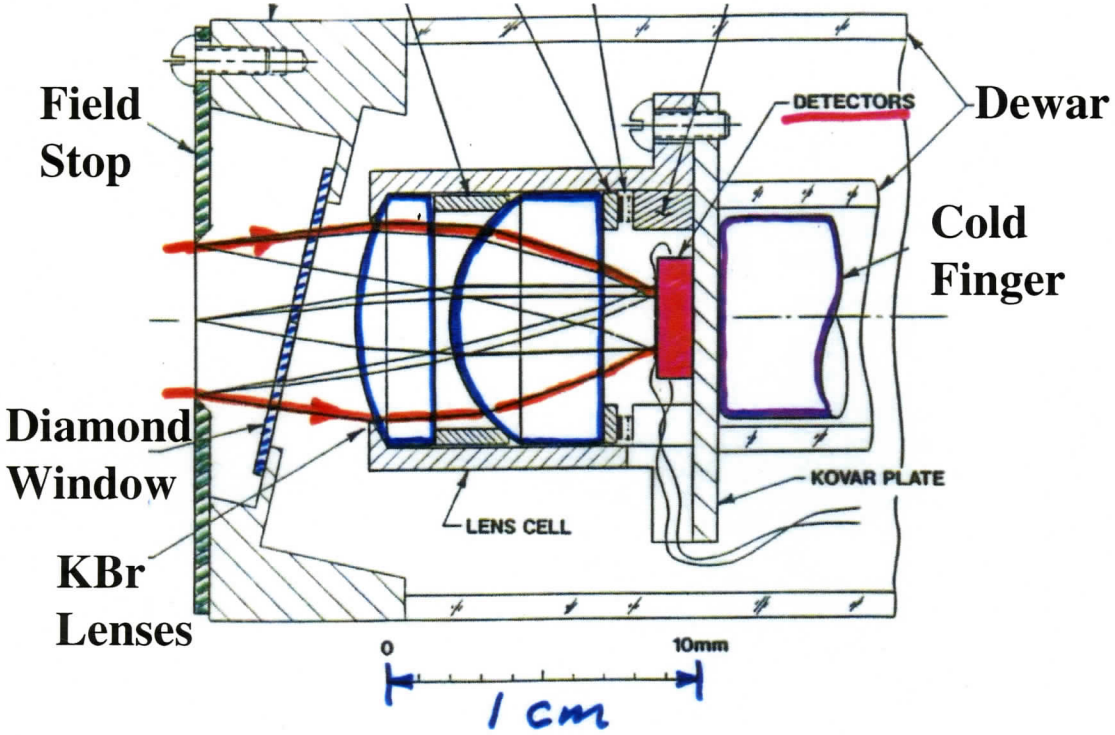

Dewar with tilted diamond window & KBr lenses

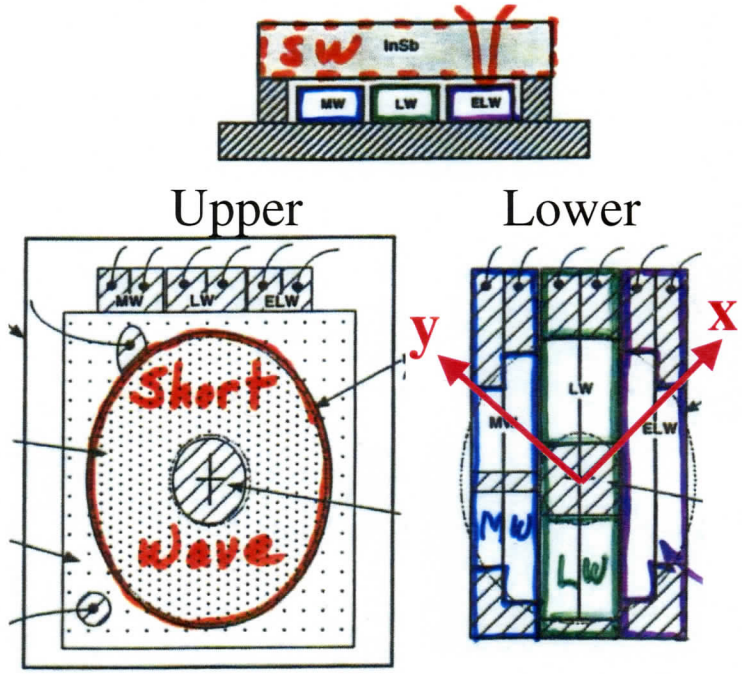

Sandwich Detectors:
Shortwave InSb on top
MW, LW, ELW below

S-HIS LW Vibration-induced Tilt Noise (caused by Sample Position Errors)

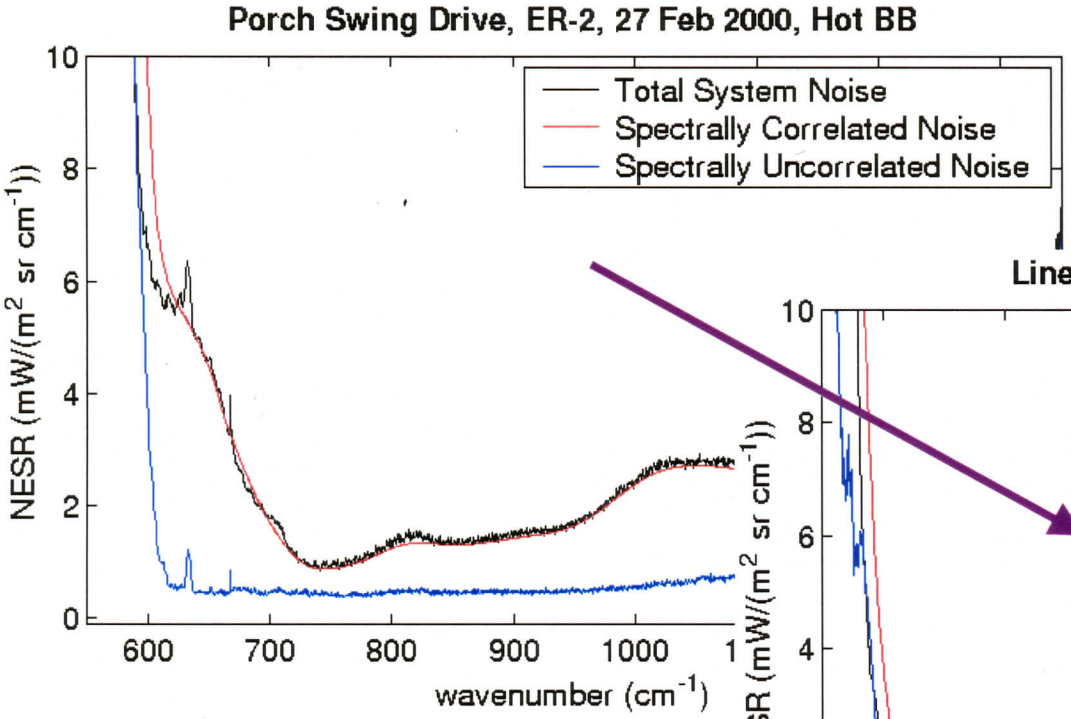

Improvement from replacing Porch Swing with Bearing OPD-Drive Mechanism

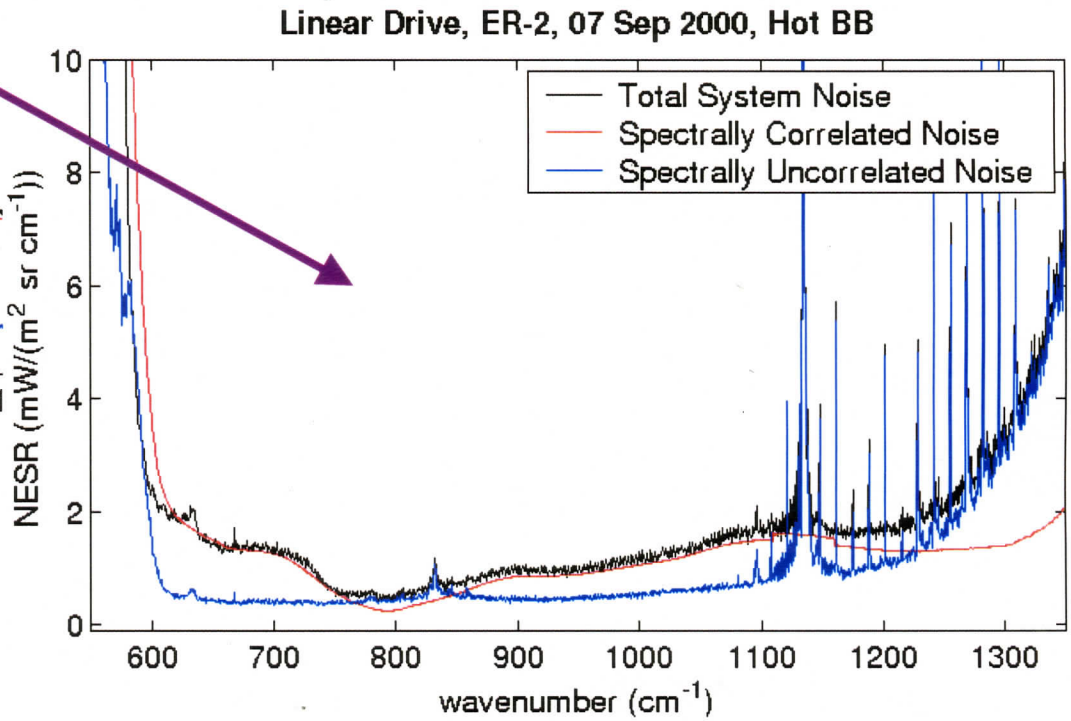

Best cases for ER2 are 2 x better, and DC8 is better yet

S-HIS LW Phase variations caused by Sample Position Errors near ZPD

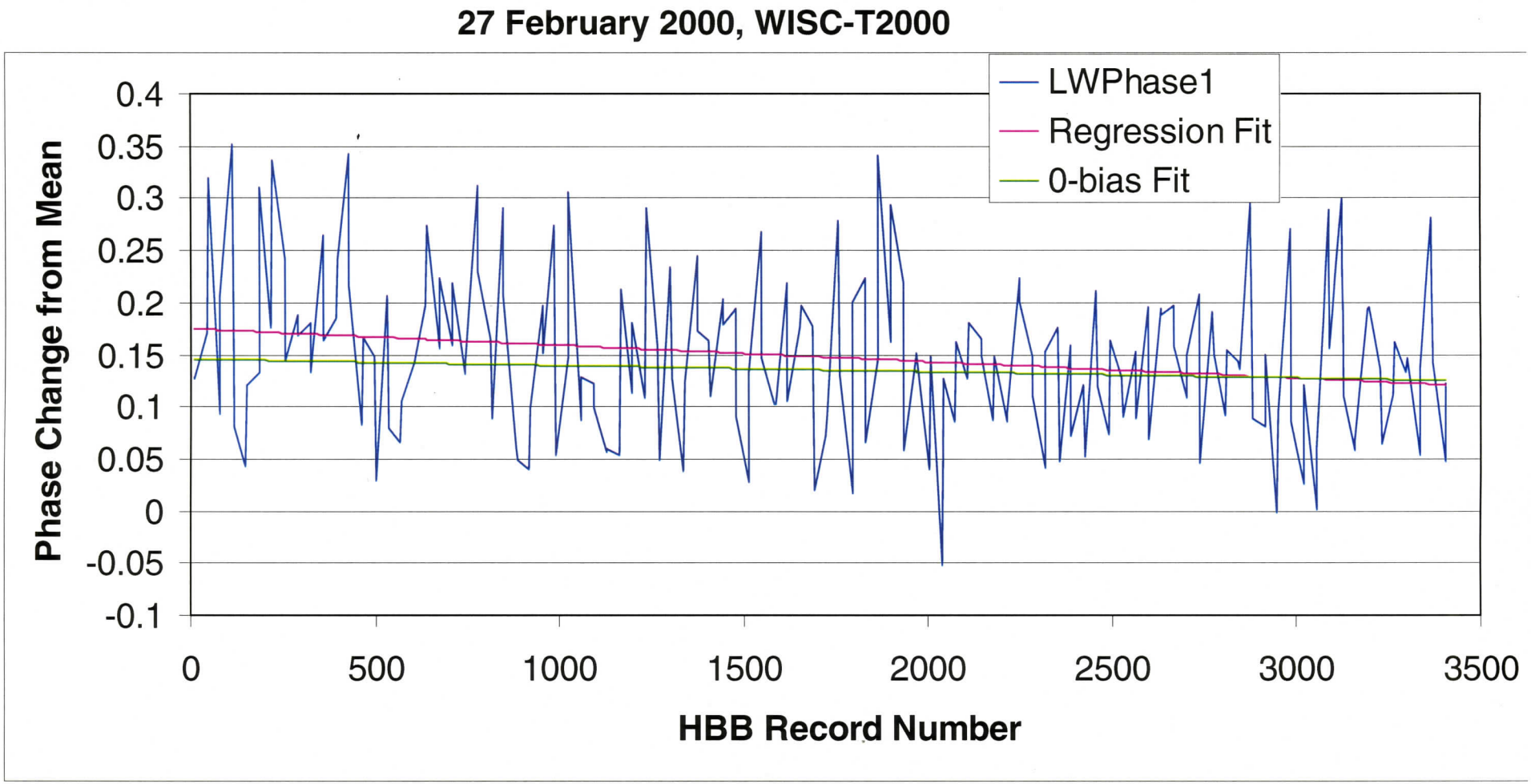

Comparison of θ_d-Tilts calculated from LW & MW Phases

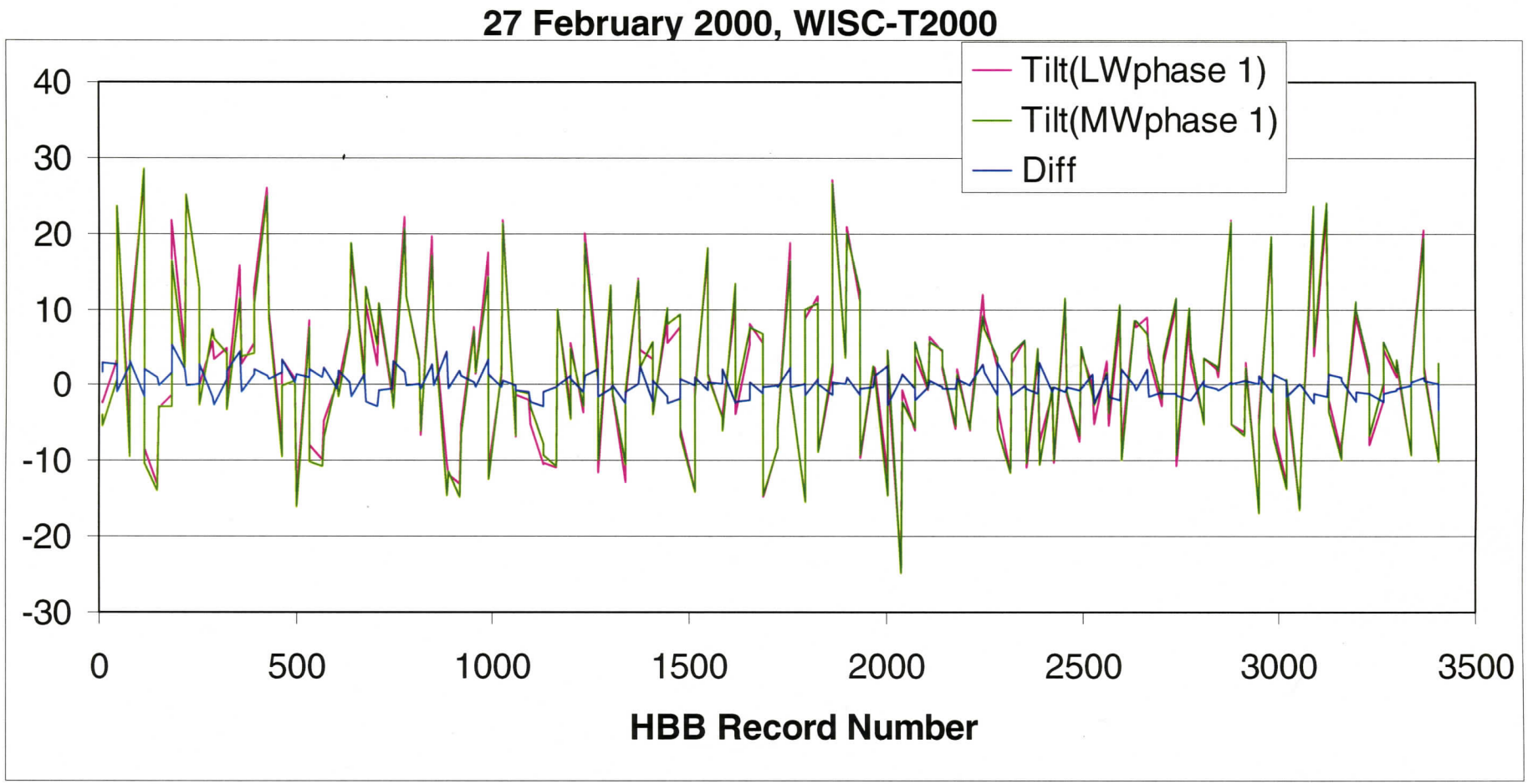

Consistency confirms part of general concept

θ_d Tilt calculated from LW Phase & from measured θ_x & θ_y tilts (γ =52°)

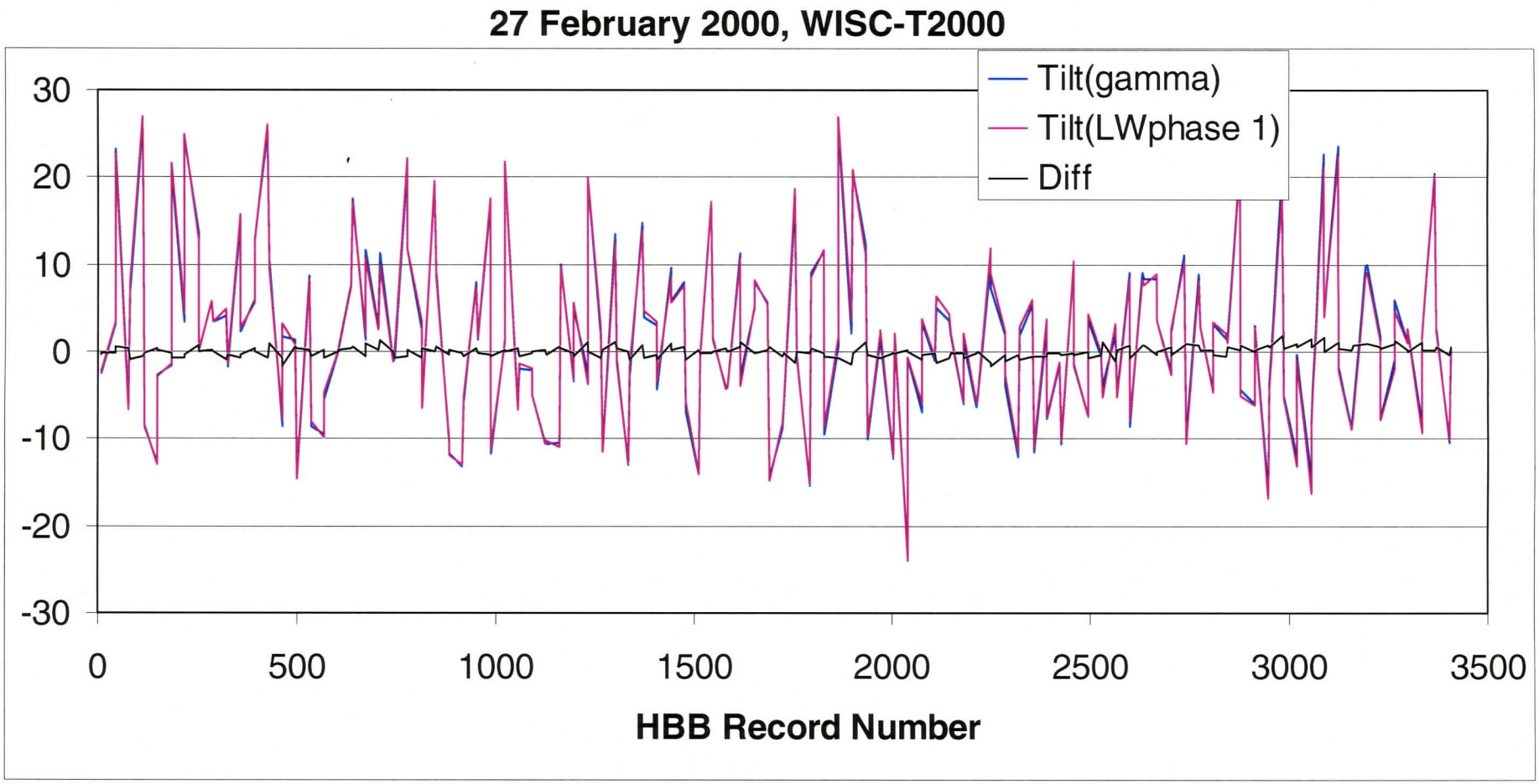

Verifies tilt measurements and concepts

θ_d Tilt calculated from MW Phase & from measured θ_x & θ_y tilts (γ =36°)

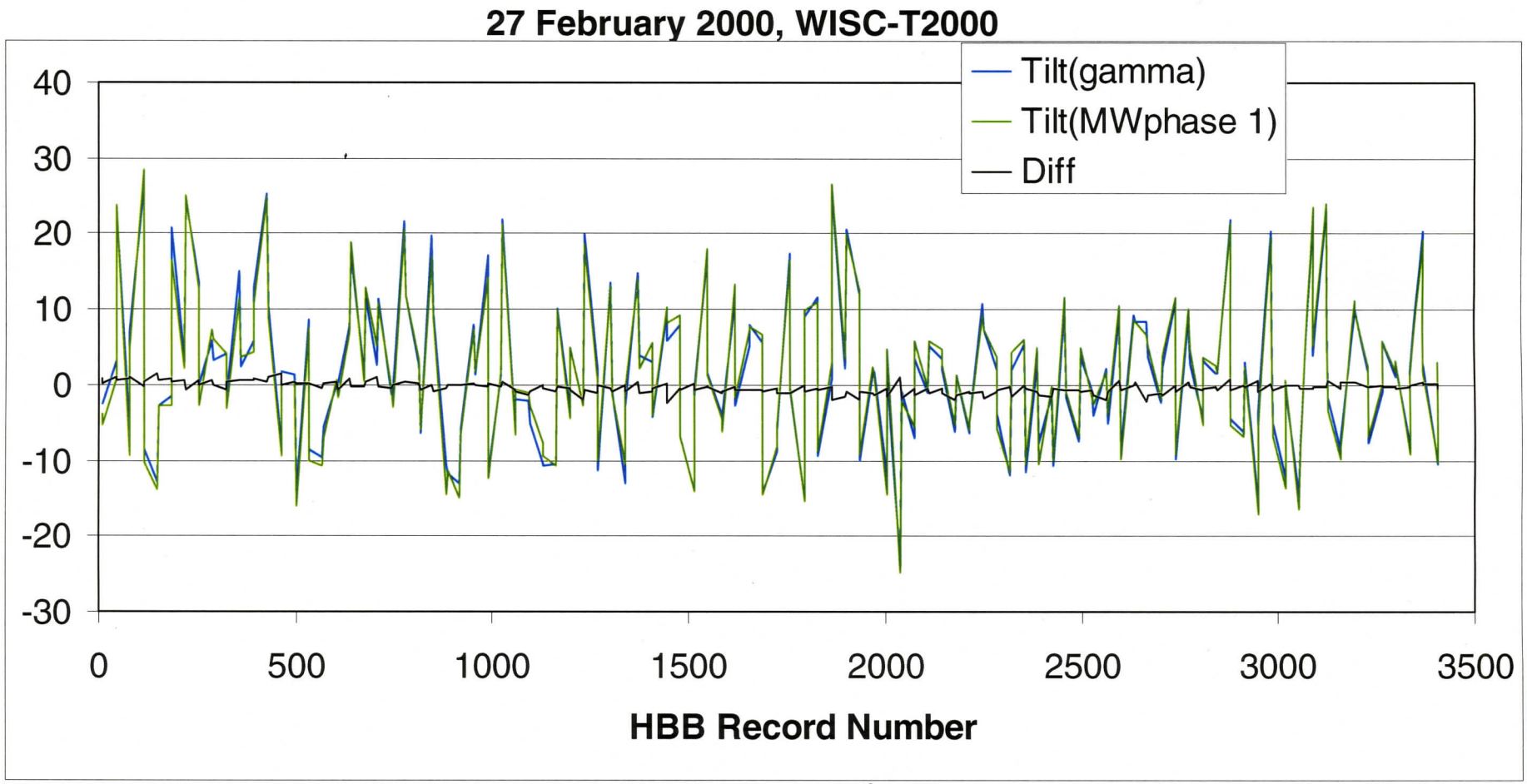

Verifies tilt measurements and concepts

Correction for Sample Position Errors

- Correction is conceptually simple:
  (1) Remove the numerical filtering and decimation
  (this results in a highly oversampled interferogram that makes accurate interpolation easy)

  (2) Modify the amplitude to account for OPD errors δx using

  $$F_c(x_i) = F(x_i) - \tfrac{1}{2}[F(x_{i+1}) - F(x_{i-1})]\,(\delta x/\Delta x) \qquad (2)$$

  where Δx is the OPD spacing between points and δx defined by Equation (1)

  (3) Fourier transform to get the corrected spectrum

❹ Tilt Issue Applicability to CrIS

- **Size of Tilts:** Much smaller vibrations for CrIS should give much smaller tilts (no mechanical cooler & aircraft vibrations are generally large)
- **Tilt-induced Modulation errors:** The large beam size (8 cm) enhances sensitivity to modulation effects
- **Sample Position Errors:** The "S-HIS effect" exists on CrIS for off-axis detectors, because the closest aperture stop (or image) is 24 cm behind the interferometer (this needs review)
- **Tilt Monitoring System:** Should be considered

❺ Principal Component Analysis for Random Noise Filtering

- **PCA - Principal Component Analysis**

  Individual spectra are expanded in Principal Components (PCs) or eigenfunctions of the covariance matrix for a set of radiance spectra

- **PCA Random Noise Filtering**

  Noise filtering results when the # PCs needed to reproduce atmospheric variance n is < total # spectral channels N

  ν -mean Noise reduction $\rightarrow \sqrt{(n/N)}$, as sample set $\rightarrow \infty$

  The approach presented here uses PCs derived from the measurement set itself

  The key for efficient noise filtering is data with limited atmospheric variations & a large statistical sample

AFWEX 10 Dec 2000 case

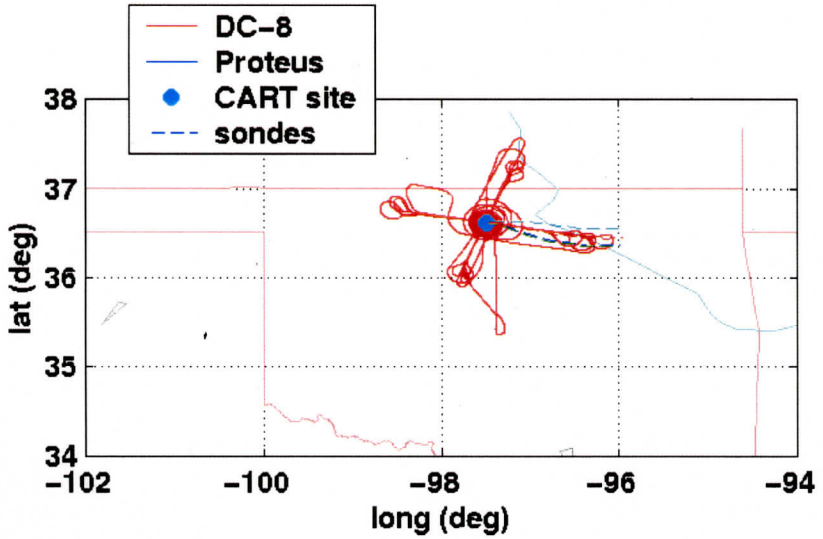

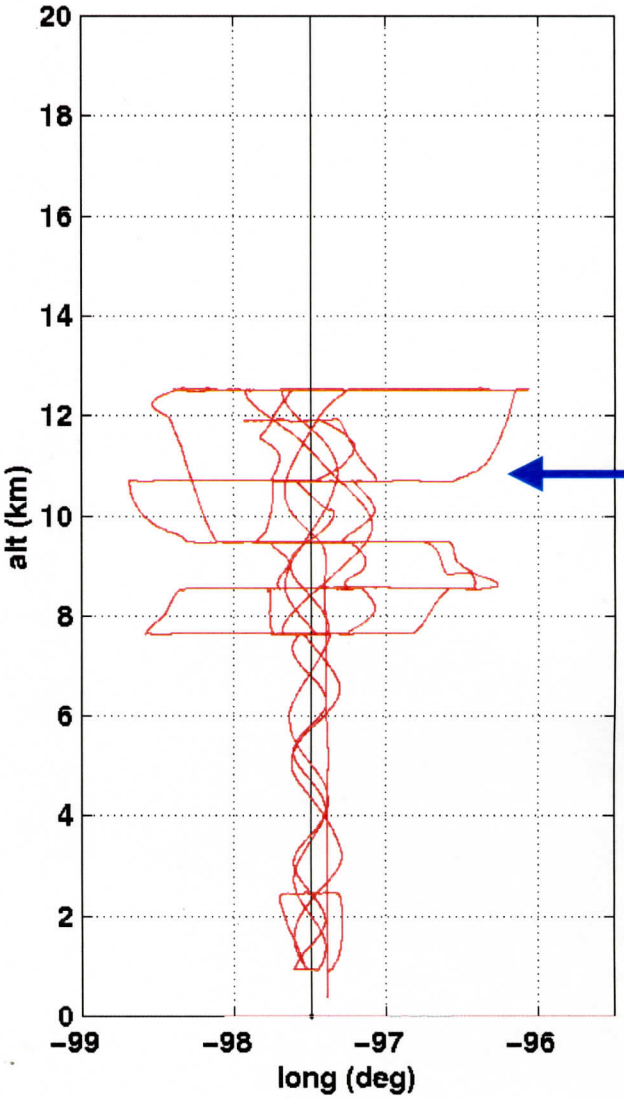

10.7 km Selected for this analysis

10.7 km

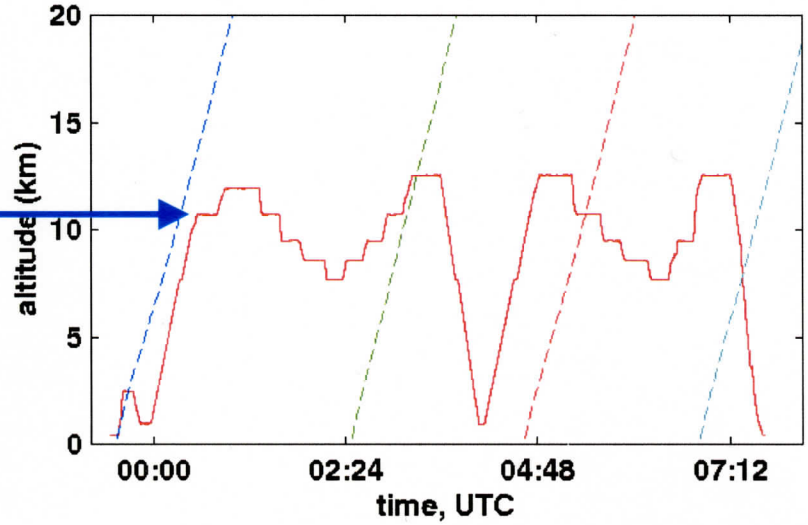

AFWEX 10 Dec 2000 case:
CART Raman Lidar Water Vapor Image

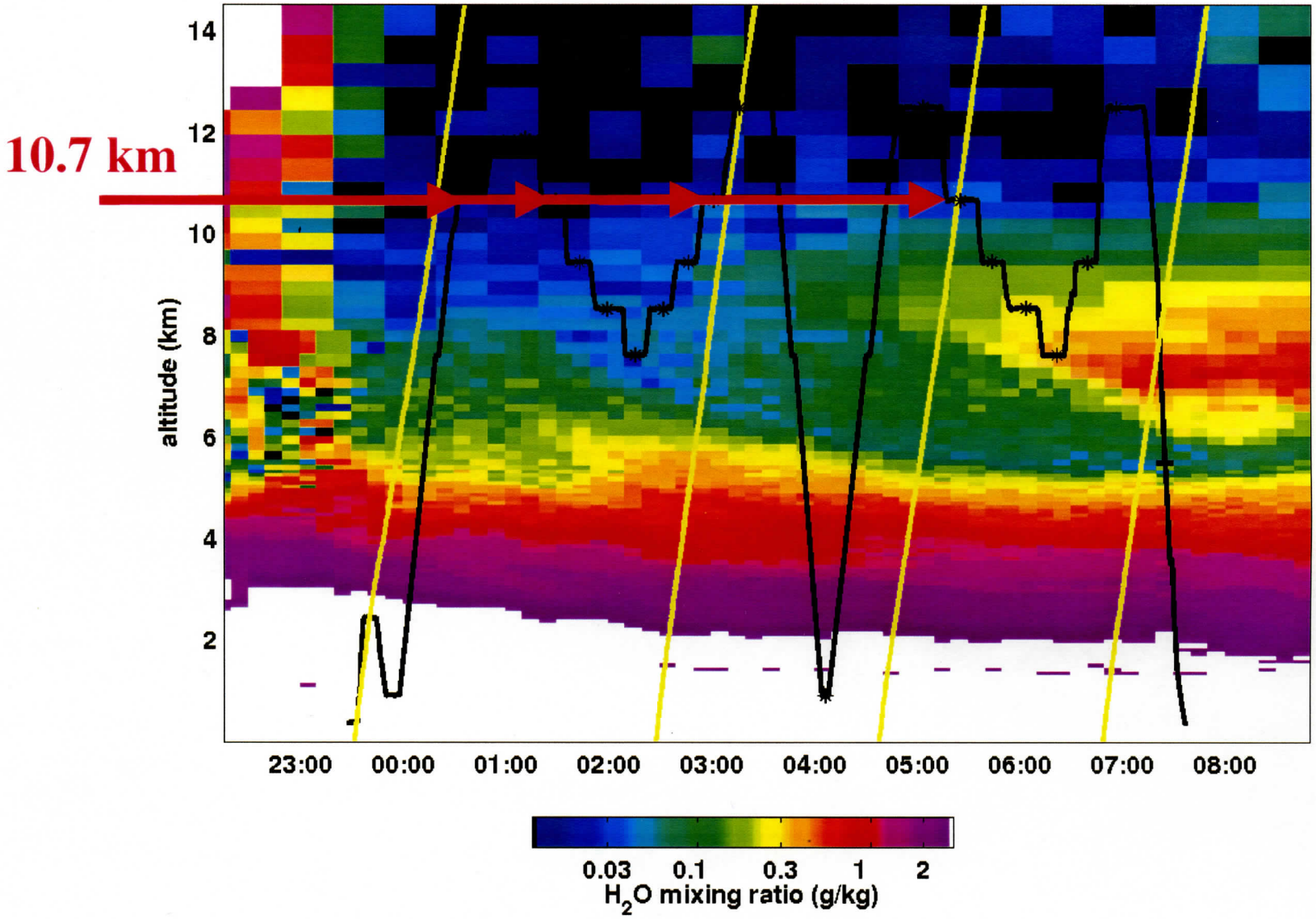

Scanning HIS PCA-Filtered Radiances

AFWEX Over ARM Central Facility, 10 December 2000

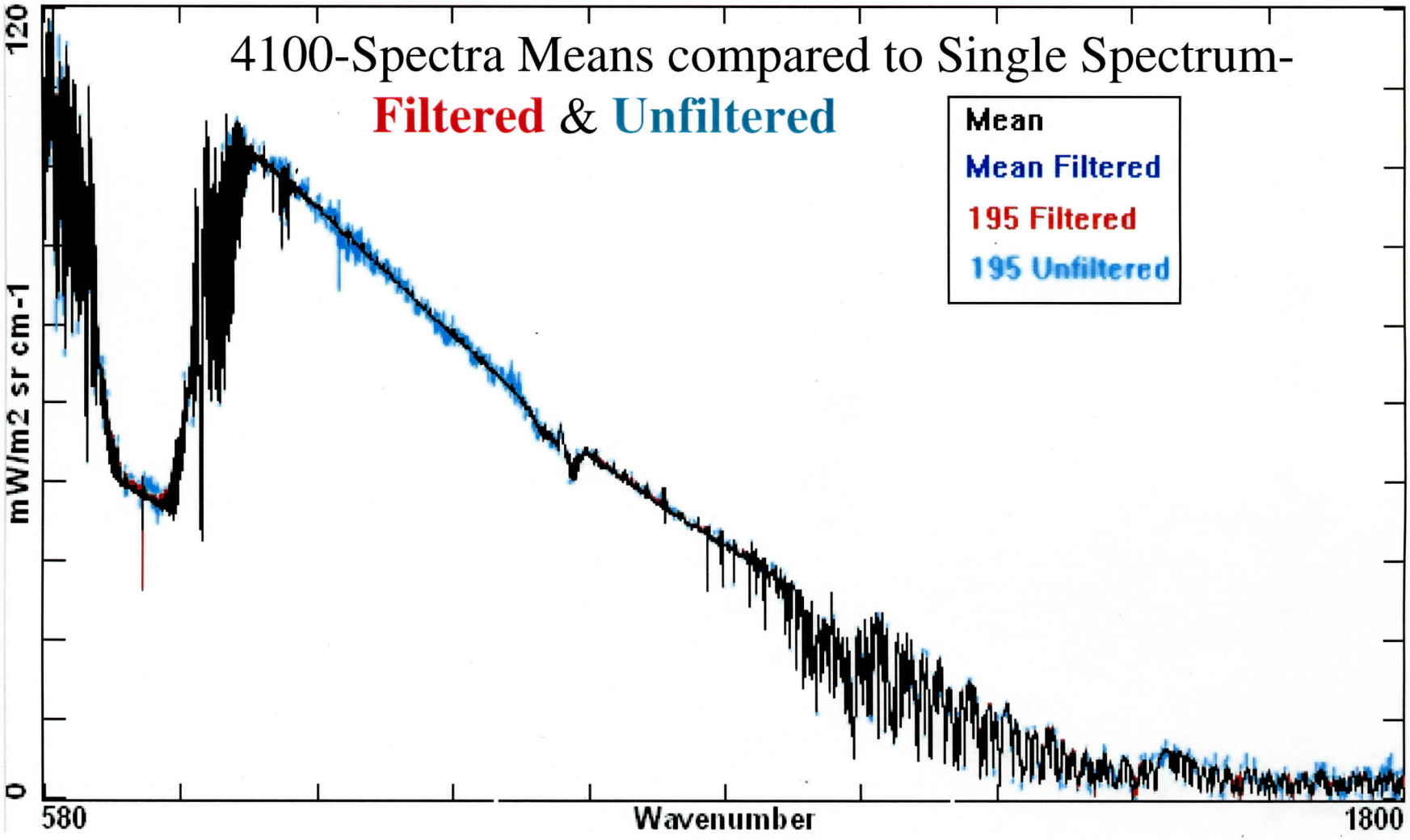

Scanning HIS PCA-Filtered Radiances

Difference of single spectrum (195) from 4100-Spectra Mean

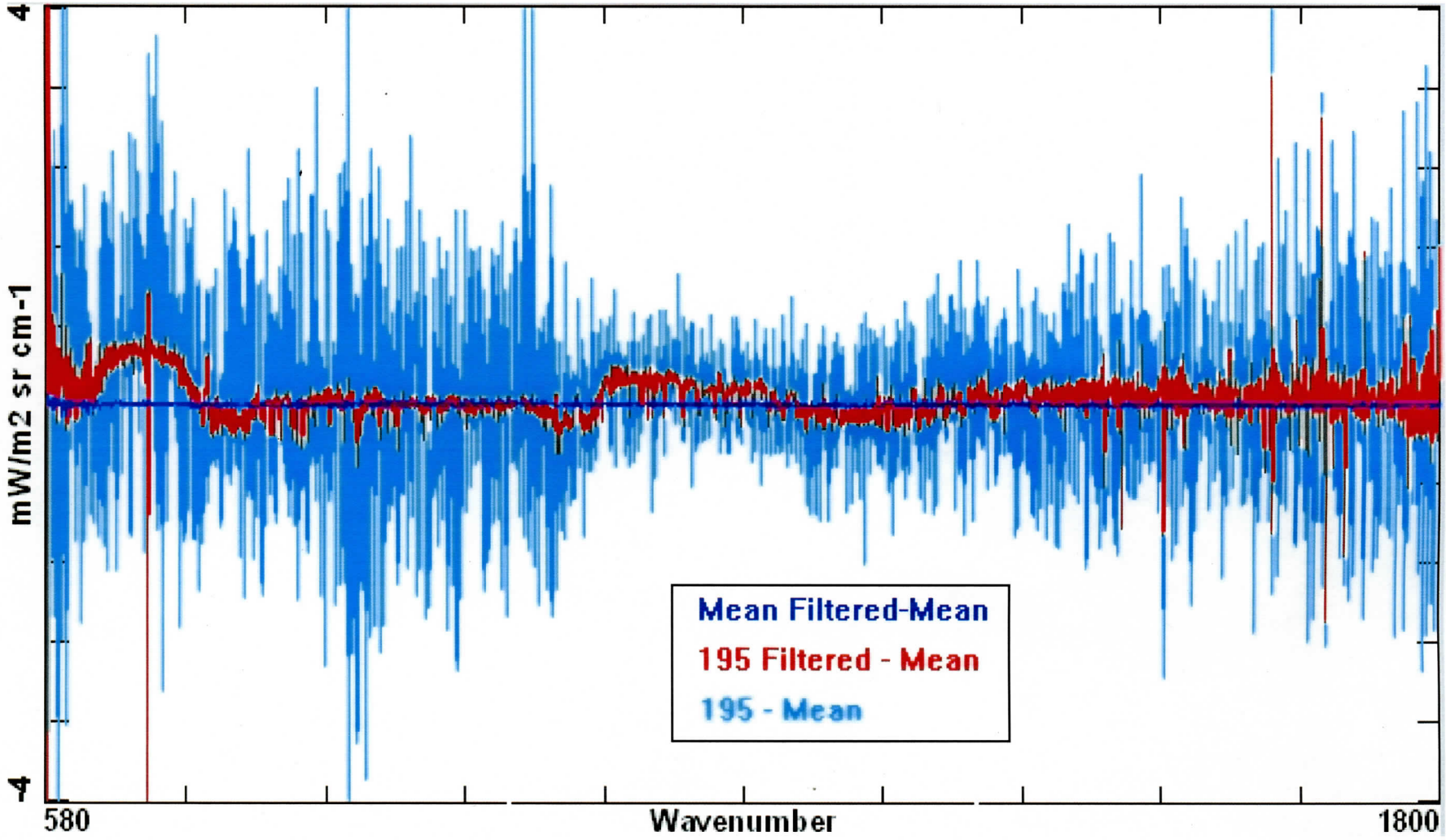

Estimate of Residual Random Noise

Standard Deviation Unfiltered & Filtered (2 estimates)

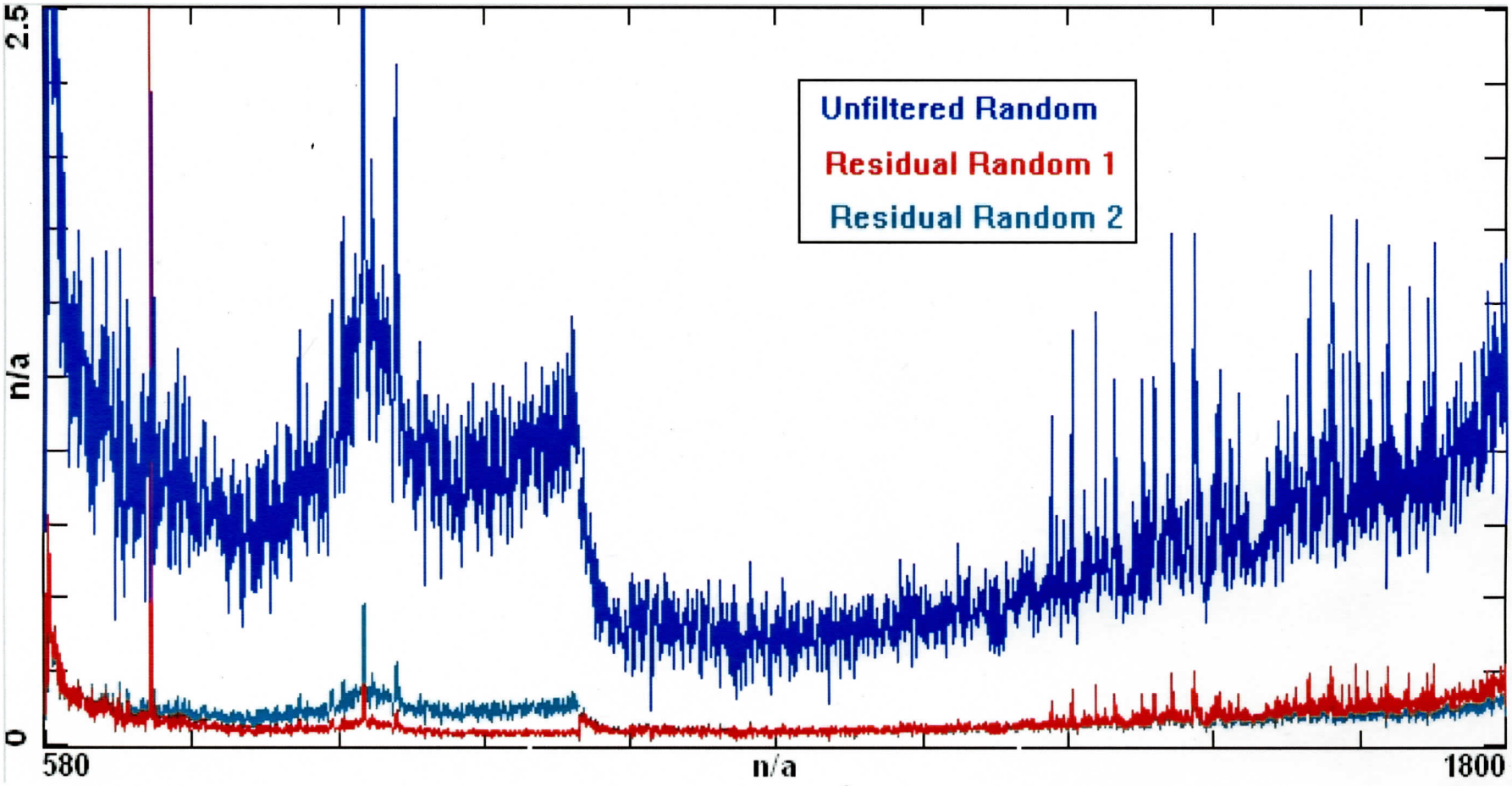

Scanning HIS PCA-Filtered Radiances

15 Micron CO_2 Band

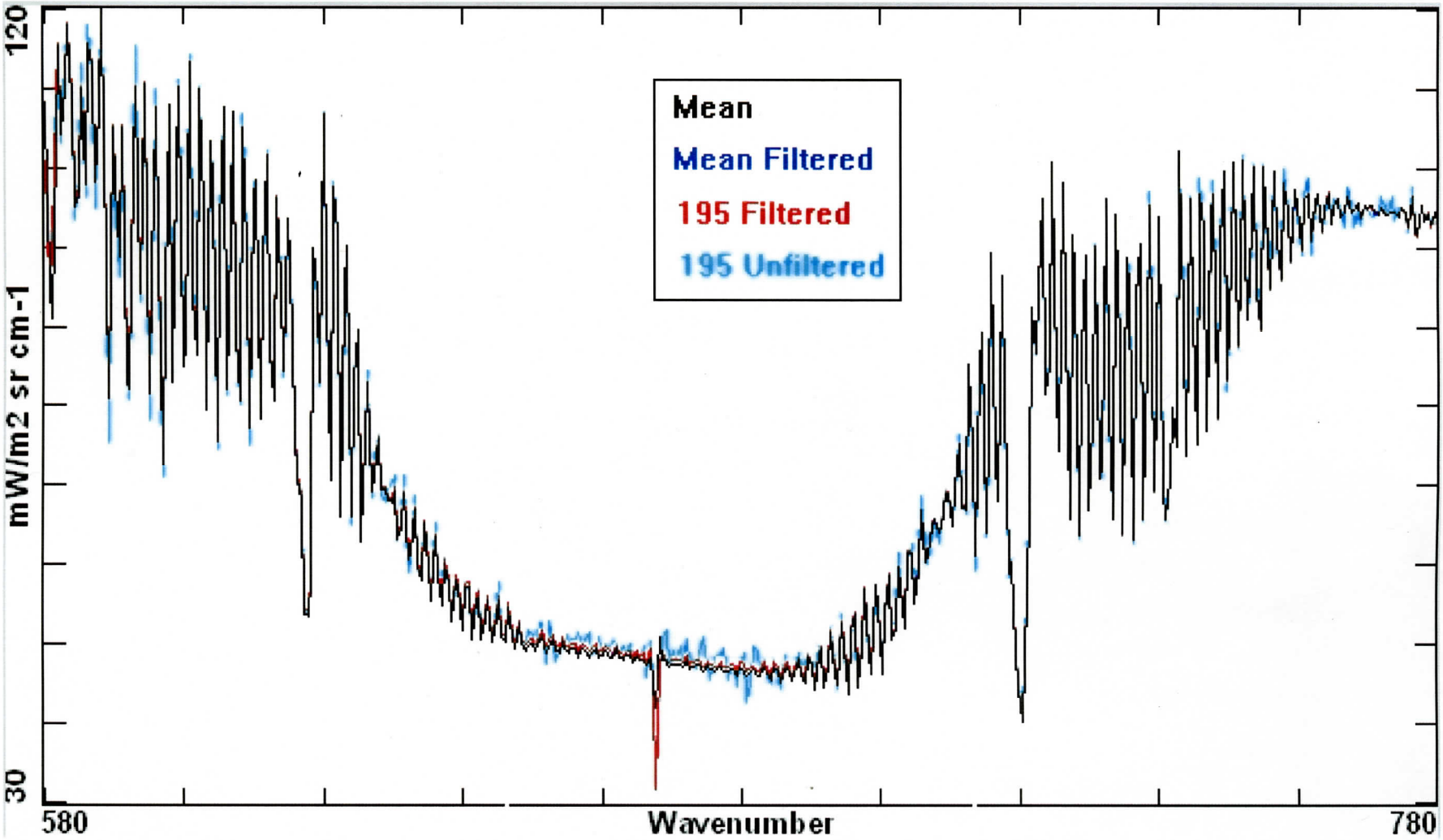

Scanning HIS PCA-Filtered Radiances

Longwave Window Region (760-850 cm^{-1})

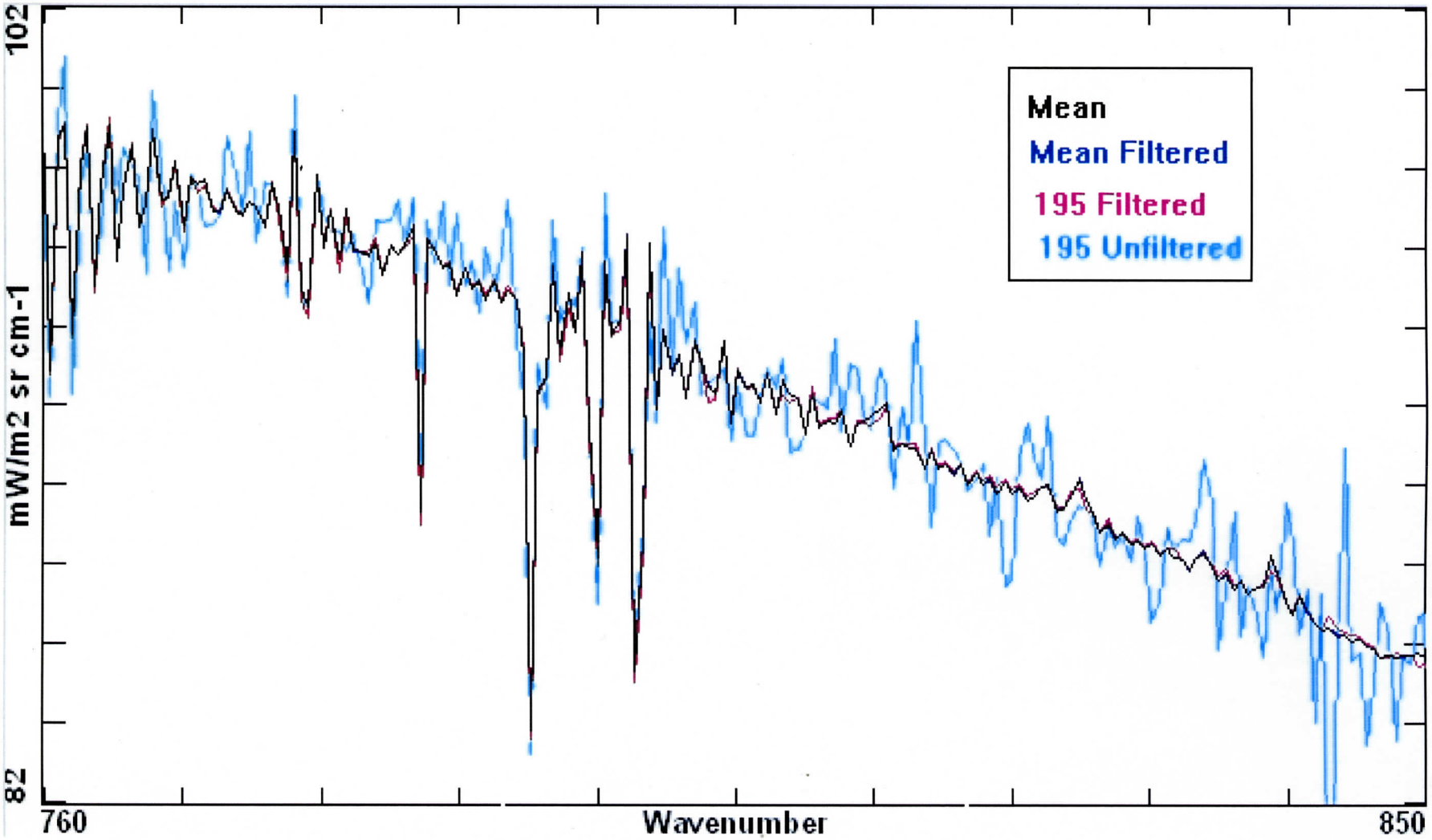

Scanning HIS PCA-Filtered Radiances

Longwave Window Region (760-850 cm^{-1}), Example 2

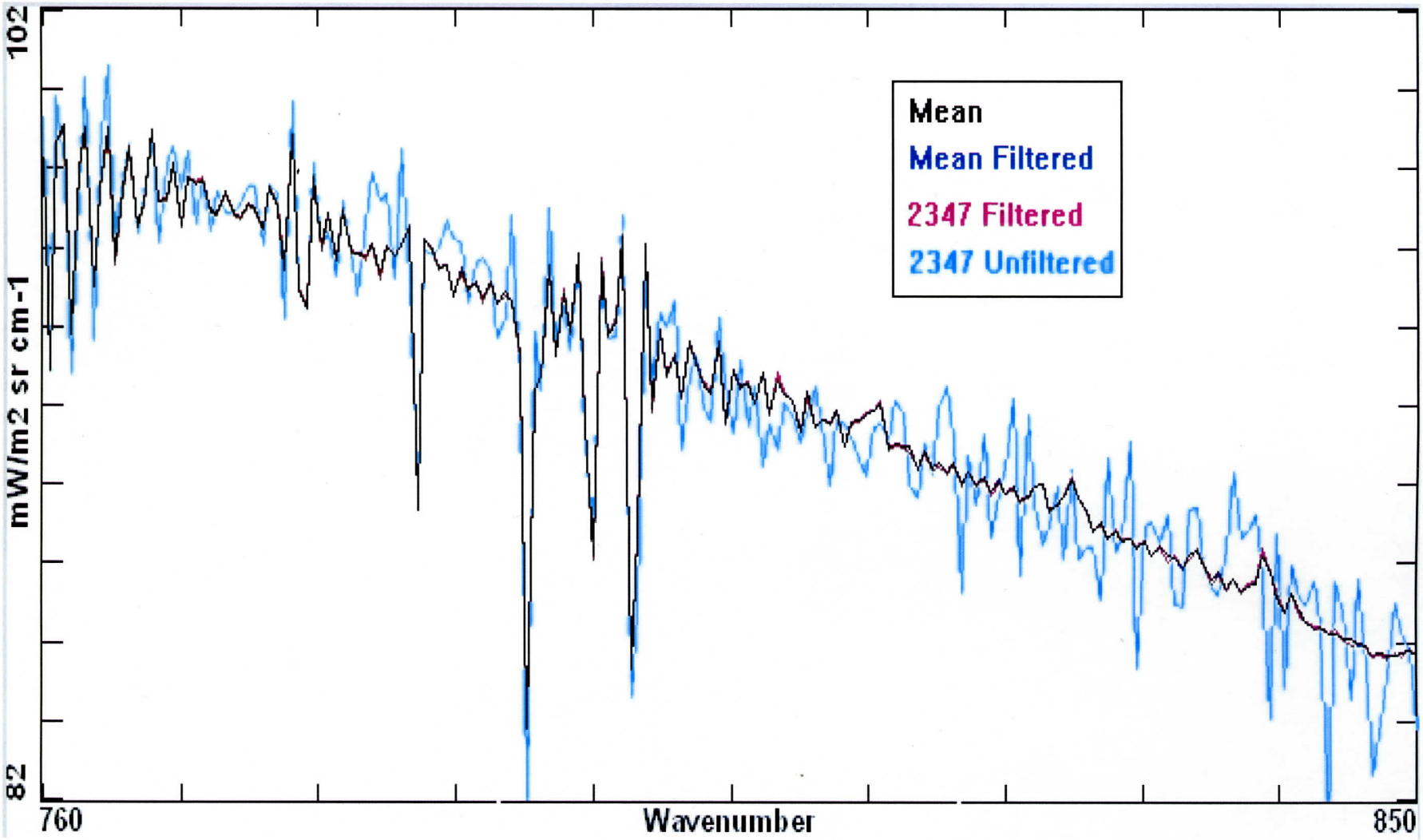

Scanning HIS PCA-Filtered Radiances

Difference of single spectrum (2347) from 4100-Spectra Mean

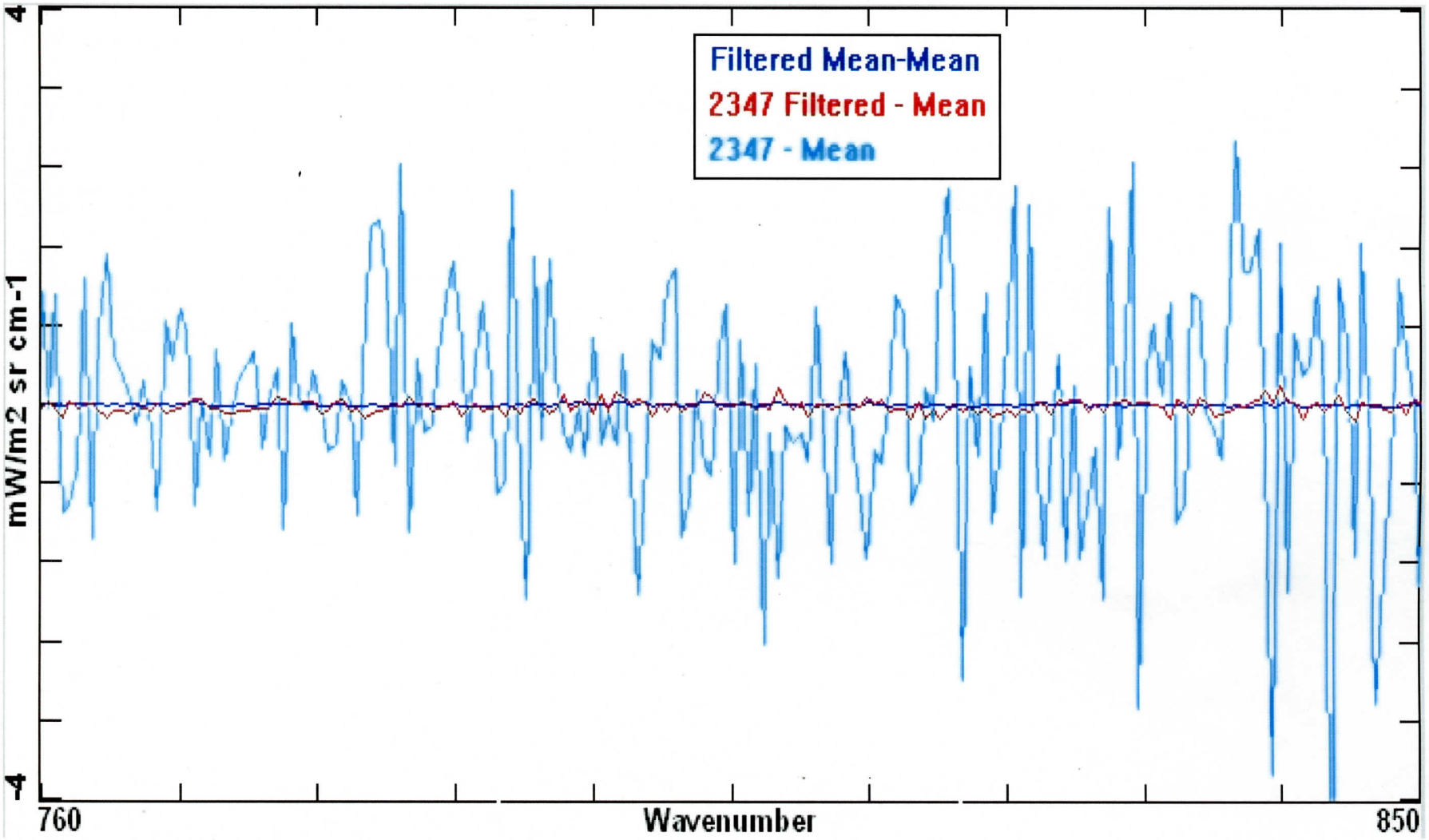

Scanning HIS PCA-Filtered Radiances

Midwave Window Region (1100-1175 cm^{-1})

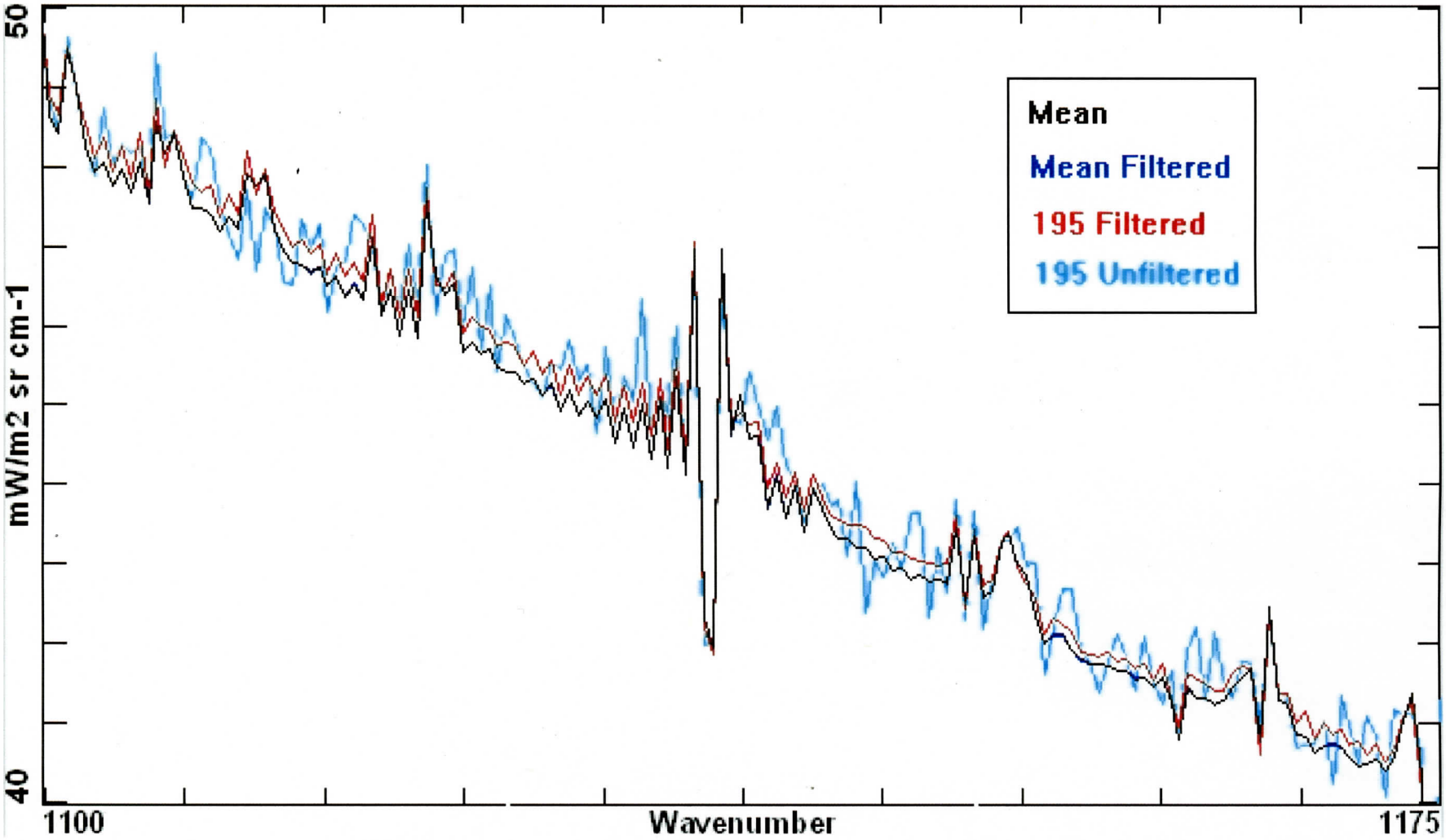

Scanning HIS PCA-Filtered Radiances

Midwave Window to Methane (1175-1325 cm^{-1})

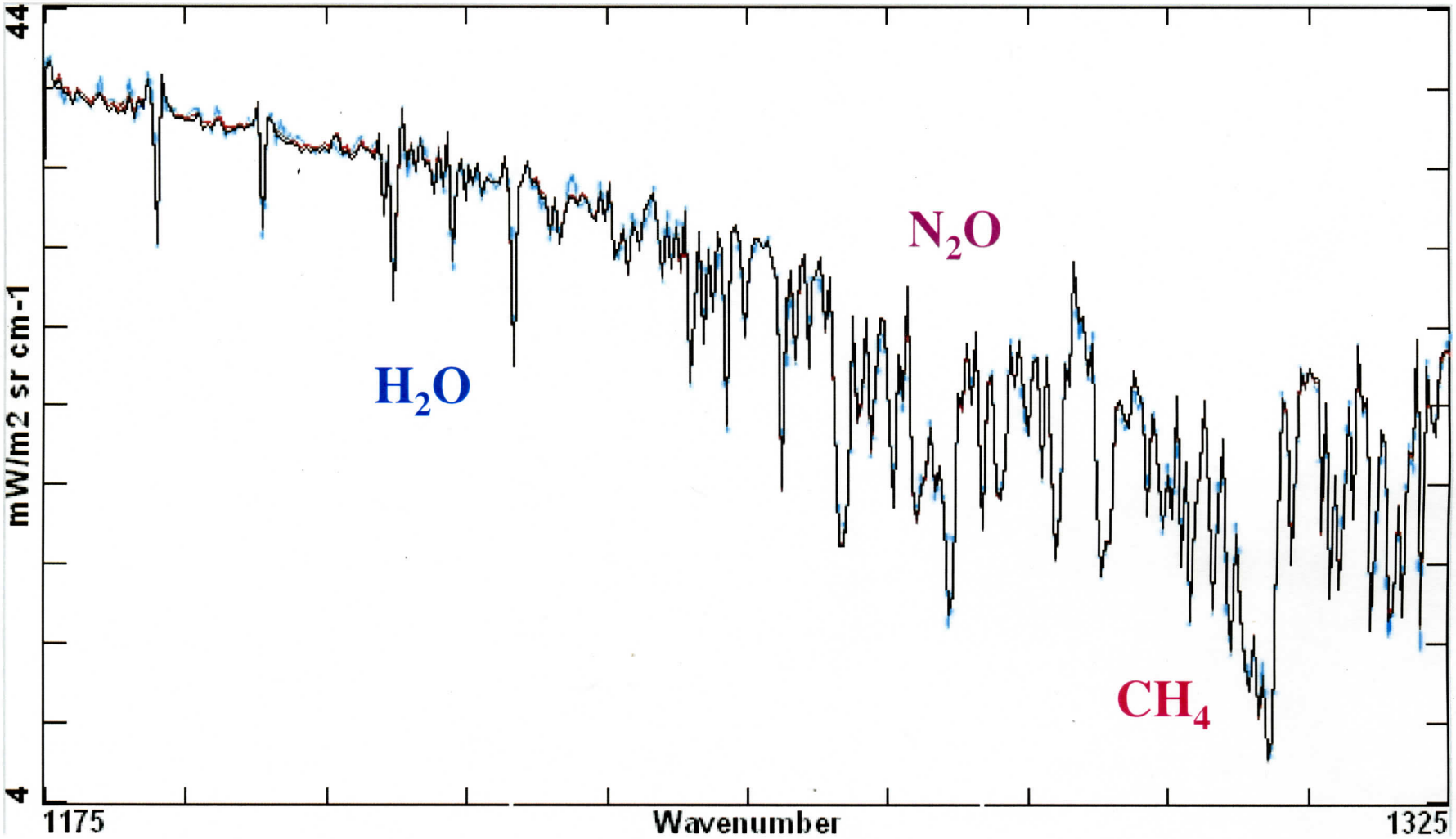

Scanning HIS PCA-Filtered Radiances

6.3 micron Water Vapor (1400-1600 cm^{-1})

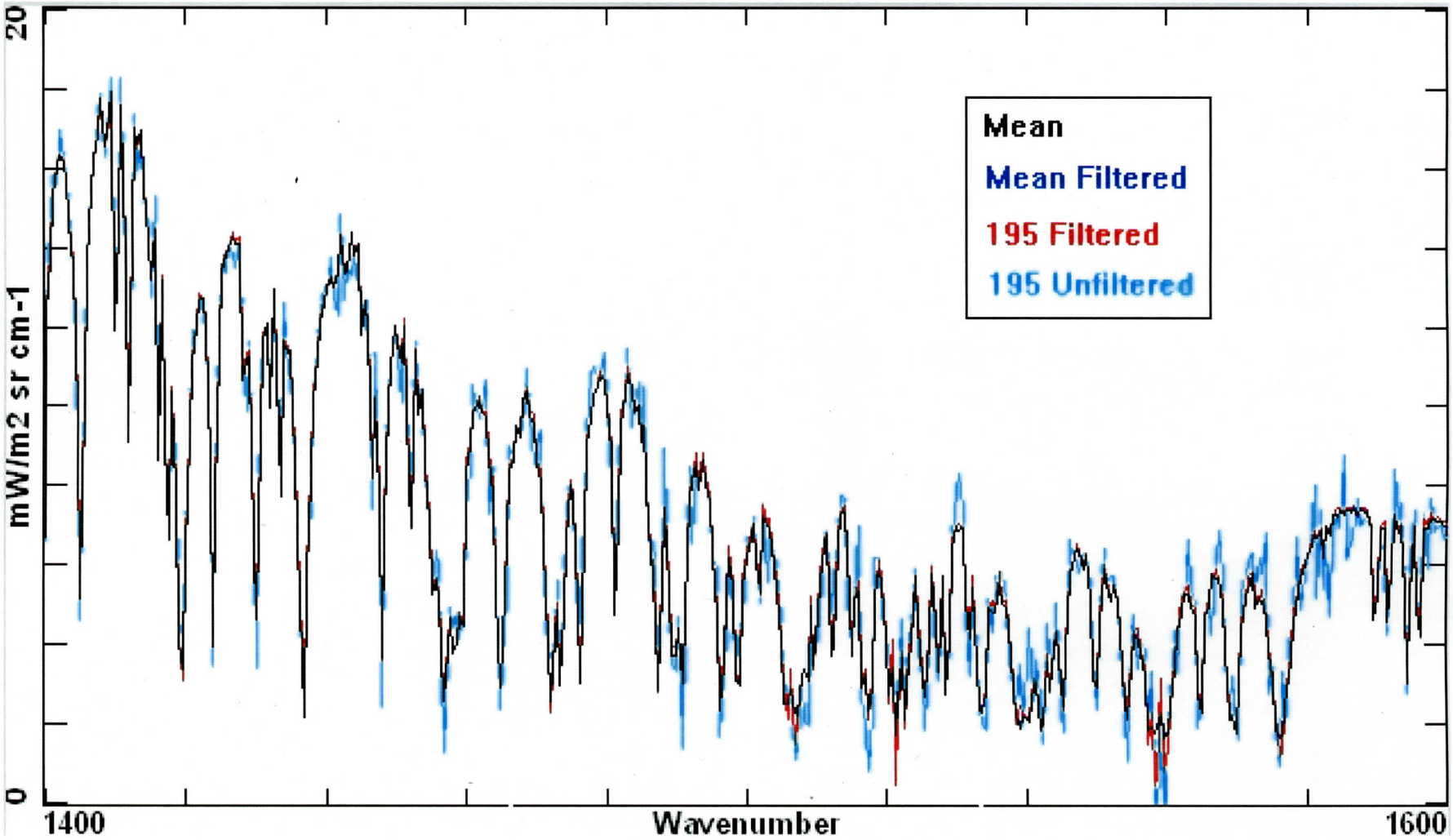

Scanning HIS PCA-Filtered Radiances

6.3 micron Water Vapor (1600-1700 cm^{-1})

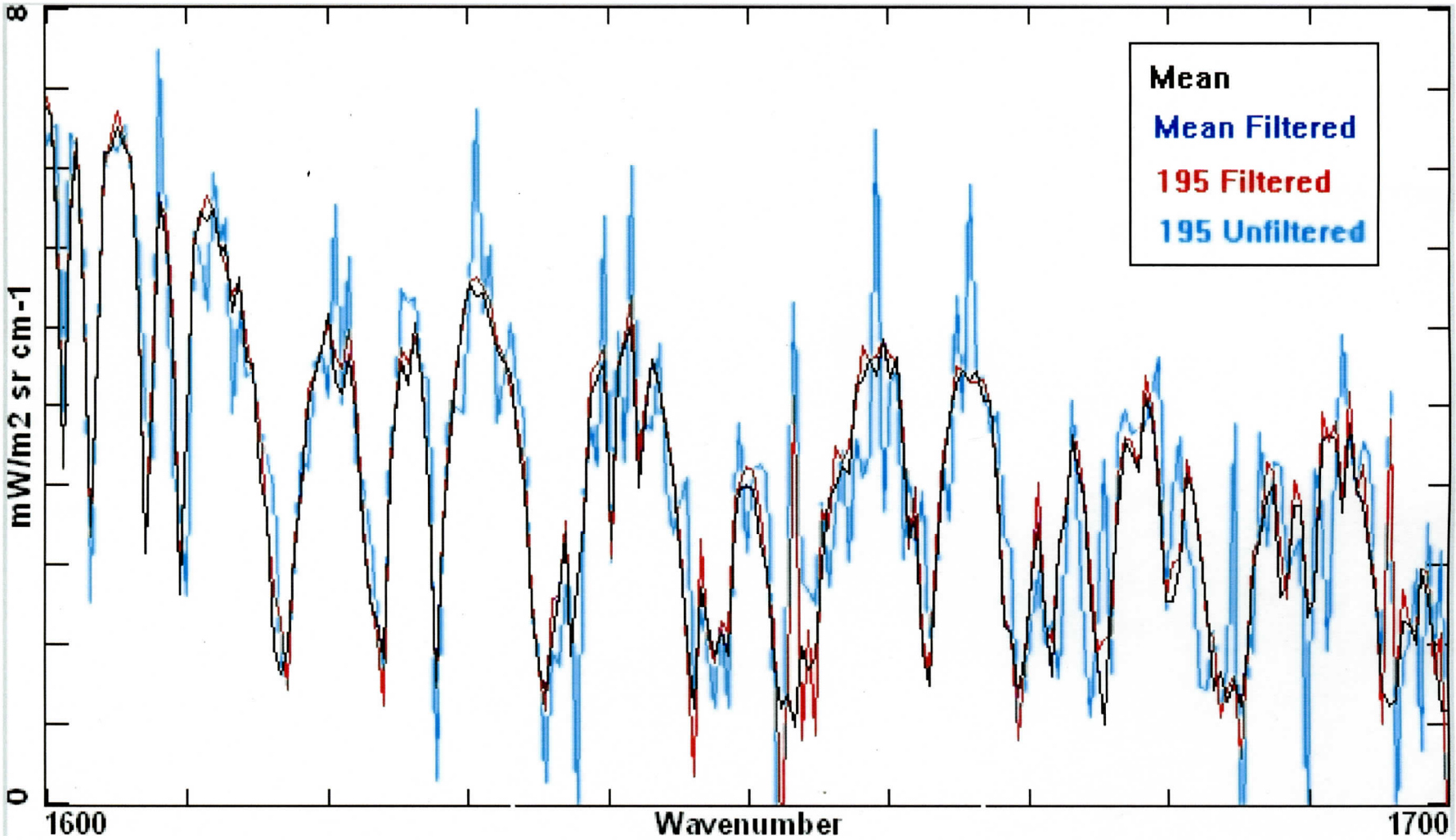

Scanning HIS PCA-Filtered Radiances

Shortwave Band (1800-3000 cm^{-1})

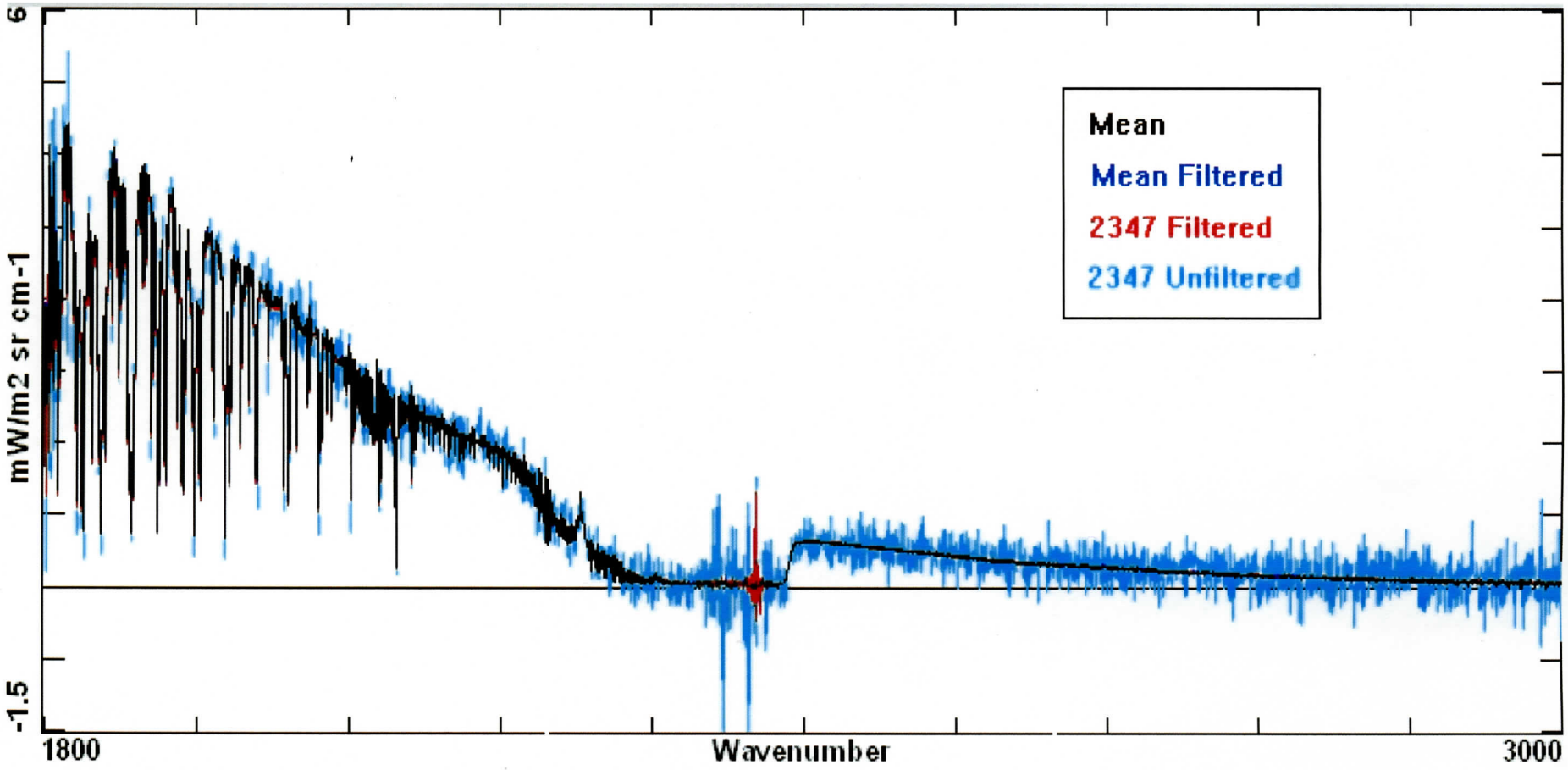

Scanning HIS PCA-Filtered Radiances

Difference of single spectrum (2347) from 4100-Spectra Mean

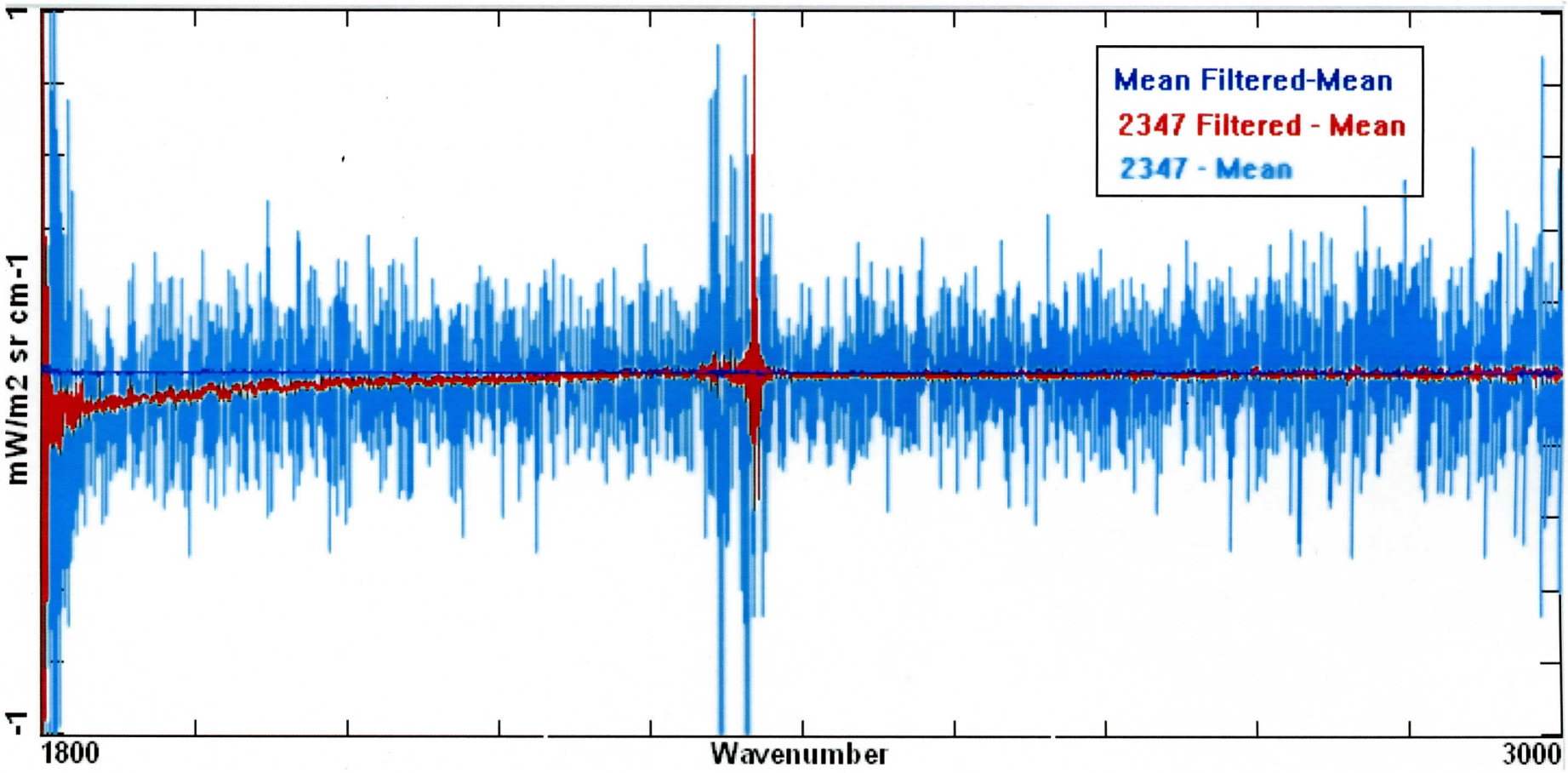

Scanning HIS PCA-Filtered Radiances

Shortwave Band (2020-2140 cm^{-1})

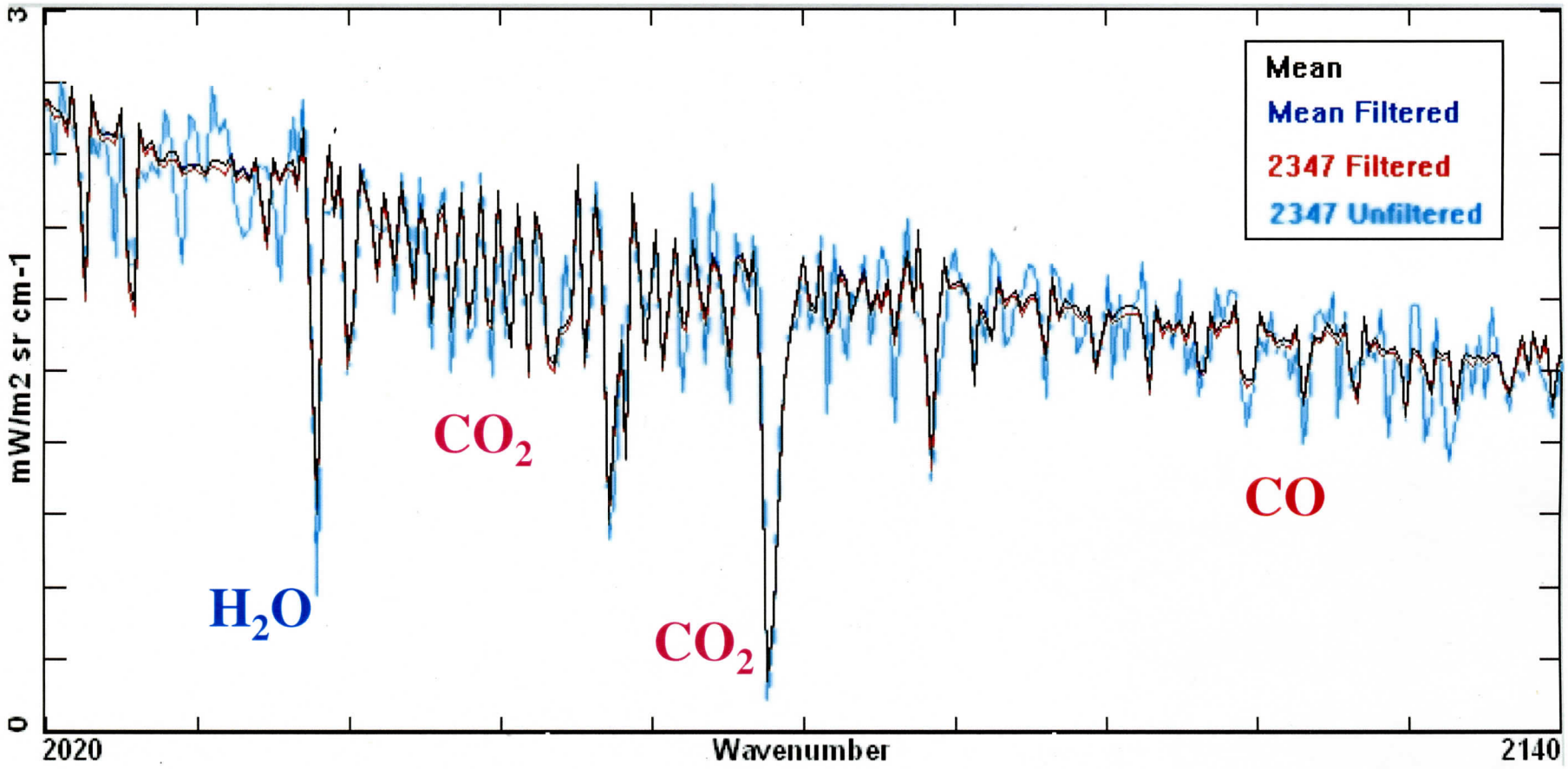

Scanning HIS 100-Spectra Means

Compared to 4100-Spectra Mean

Filtered

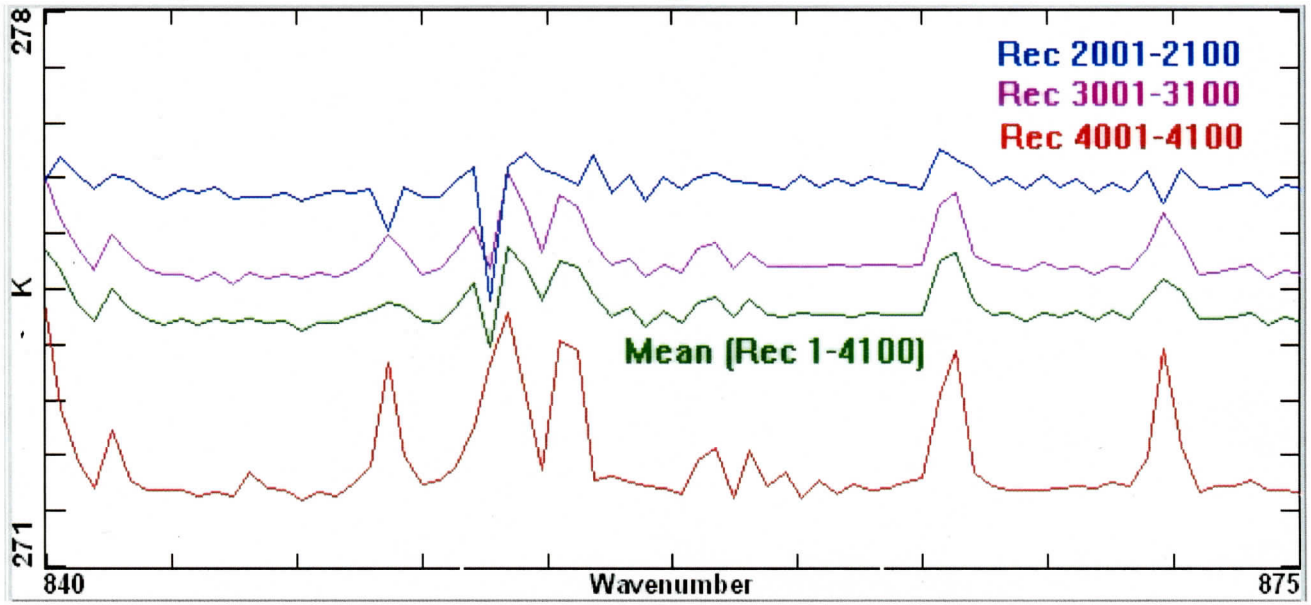

Unfiltered

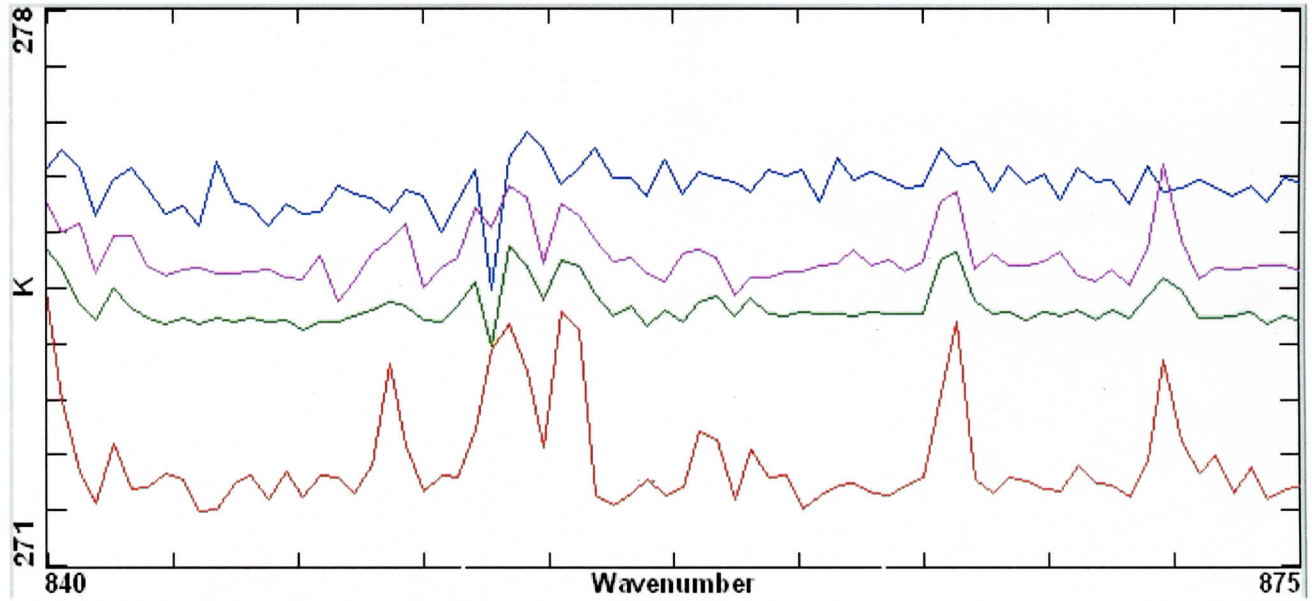

Scanning HIS 100-Spectra Means

Compared to Selected Individual Filtered Spectra

Filtered (Single Spectra)

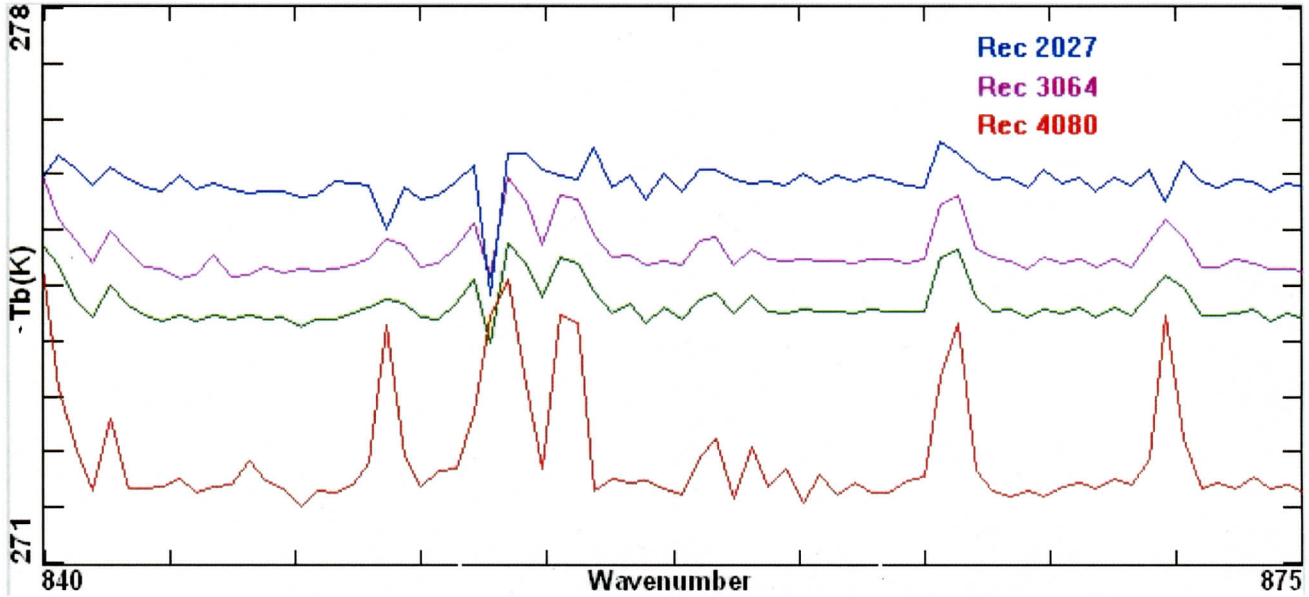

Unfiltered

Implies Filter noise reduction > factor of 10!

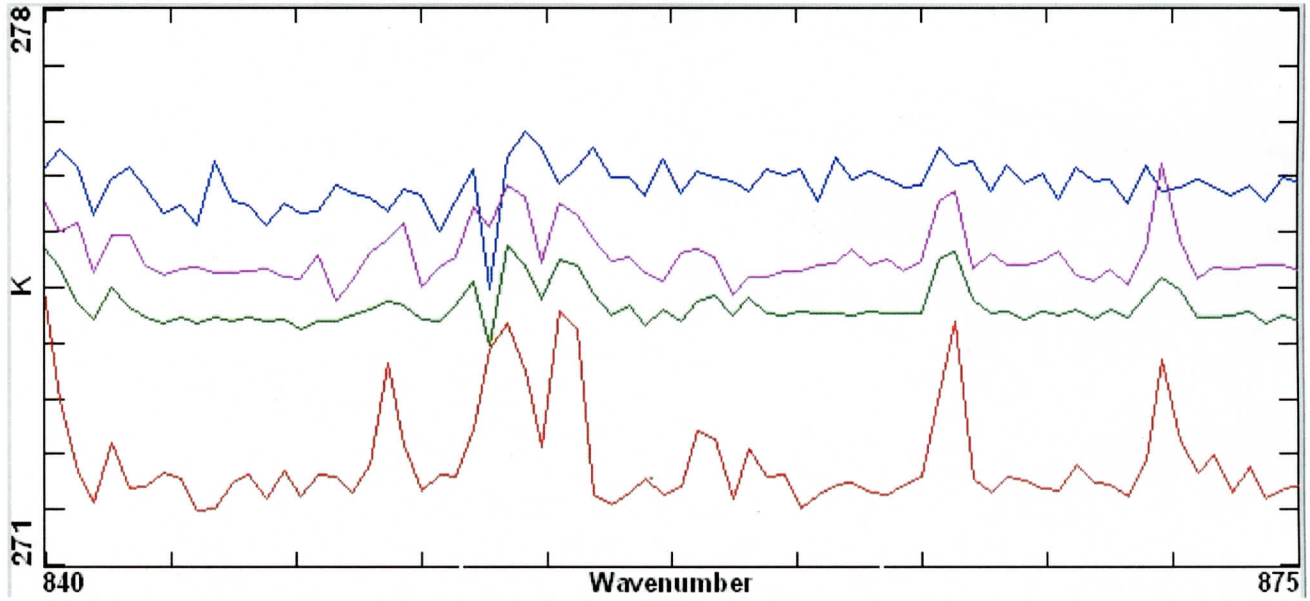

Calculation from Sonde Compared to S-HIS Brightness T Spectra

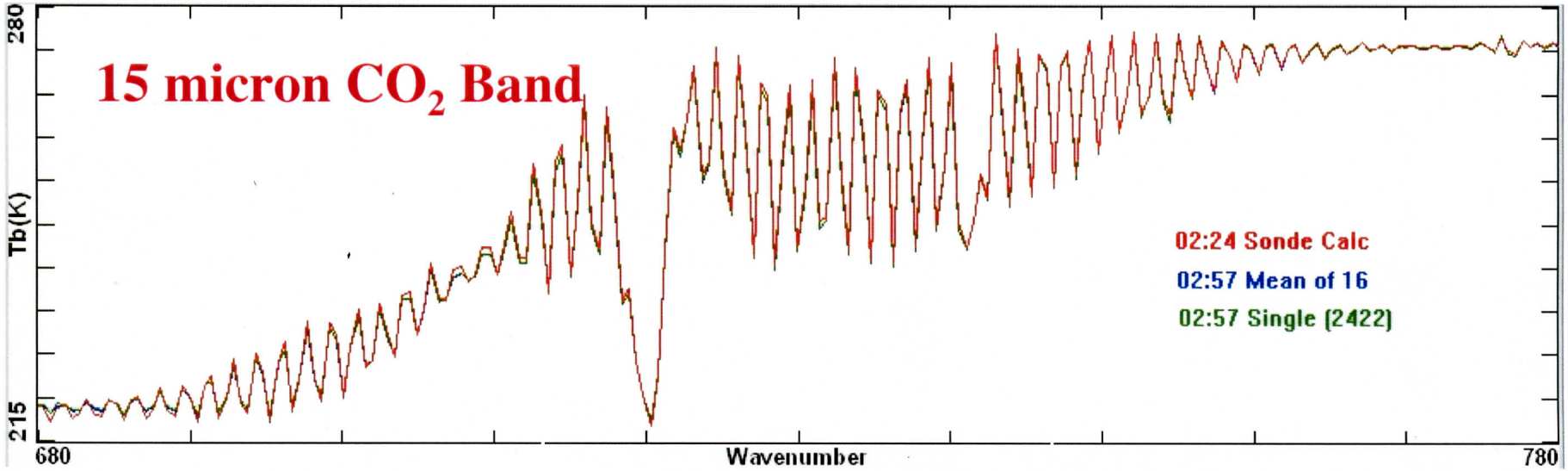

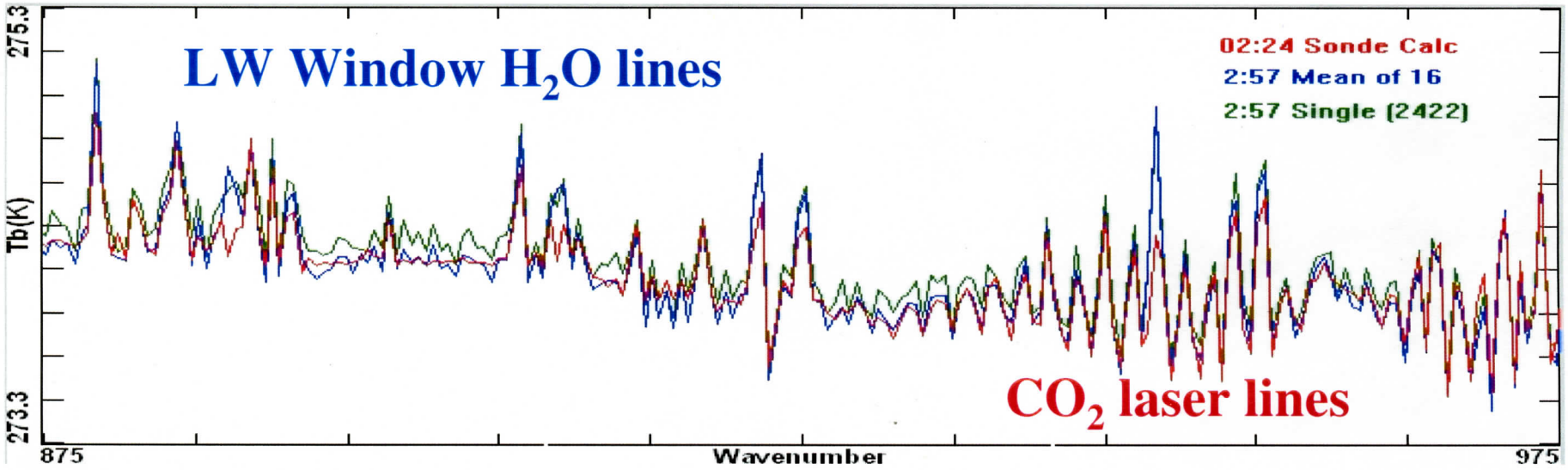

12-10-00 AFWEX

Calculation from Sonde Compared to S-HIS Brightness T Spectra

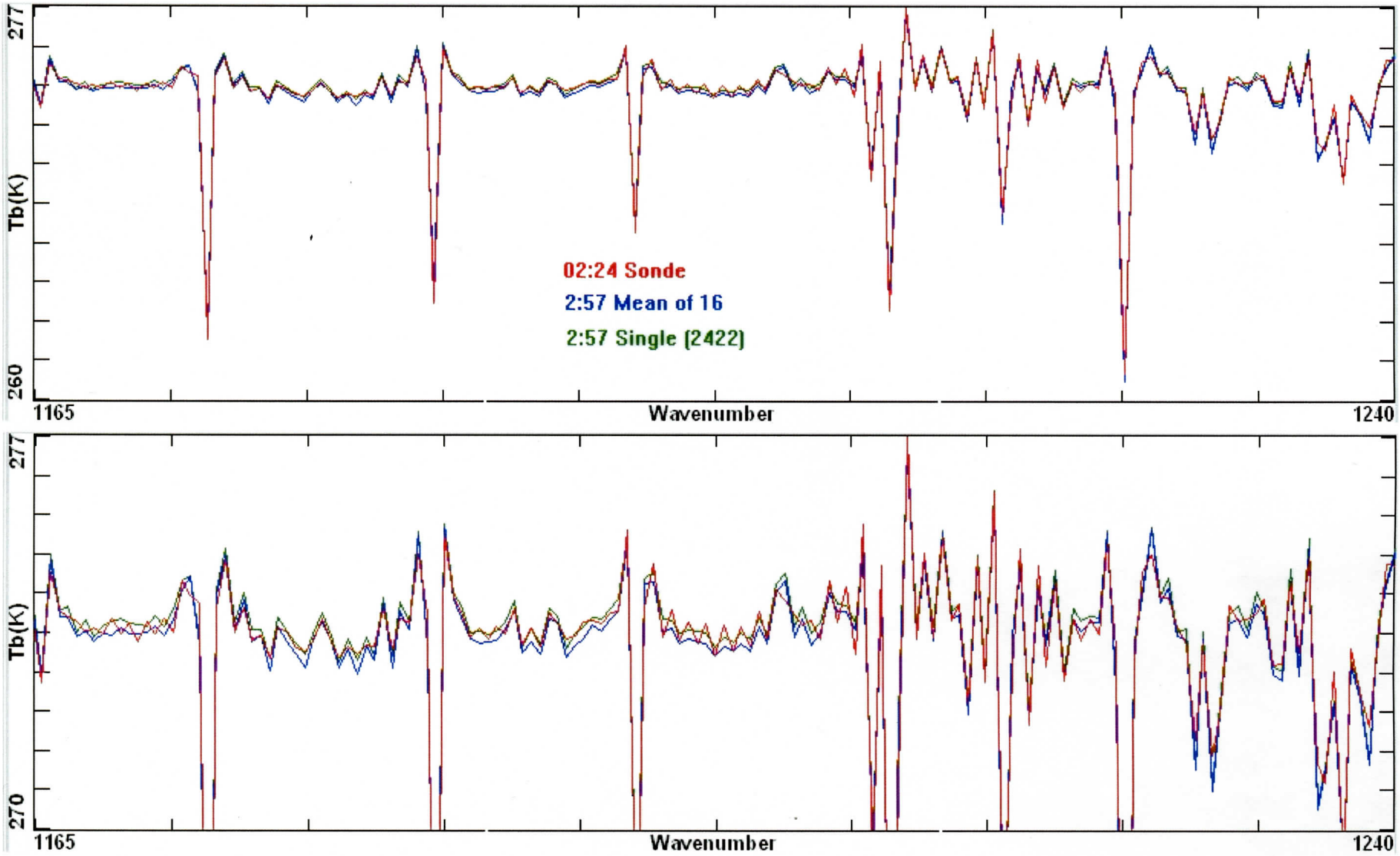

12-10-00 AFWEX

Calculation from Sonde Compared to S-HIS Brightness T Spectra

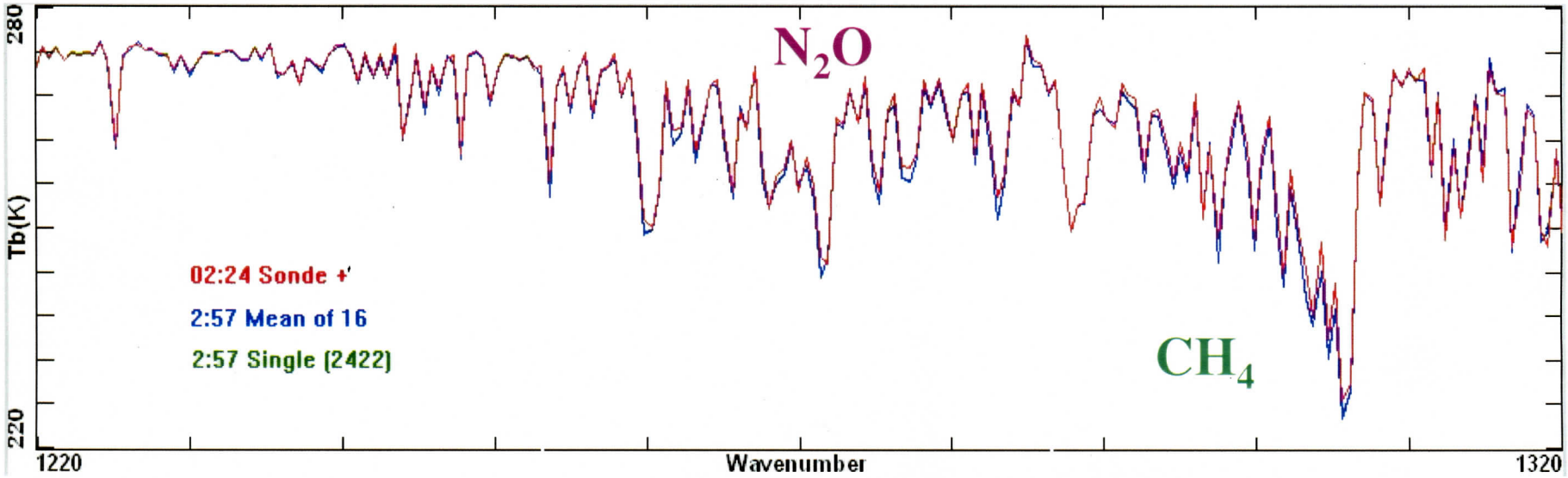

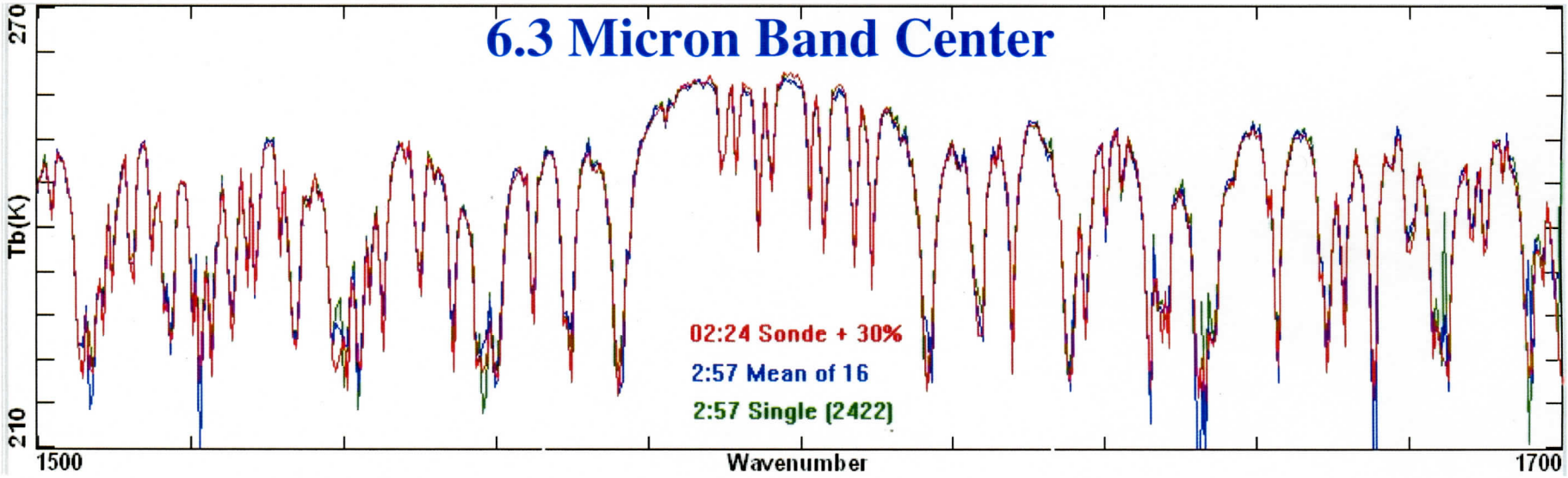

12-10-00 AFWEX

Calculation from Sonde Compared to S-HIS Brightness T Spectra

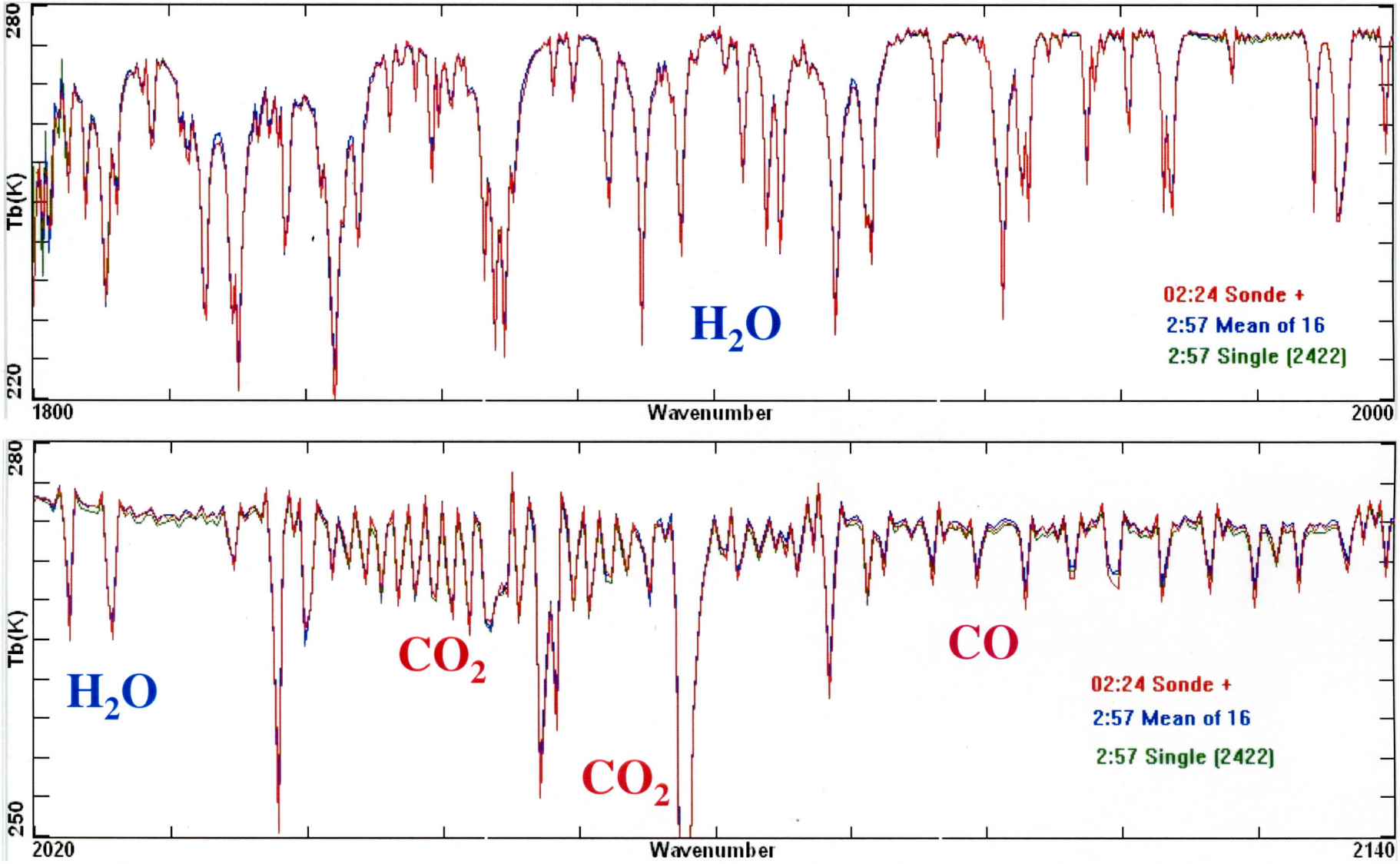

12-10-00 AFWEX

100 Single S-HIS Brightness T Spectra

Random Noise-Filtered and Unfiltered (Rec 4001-4100)

Filtered

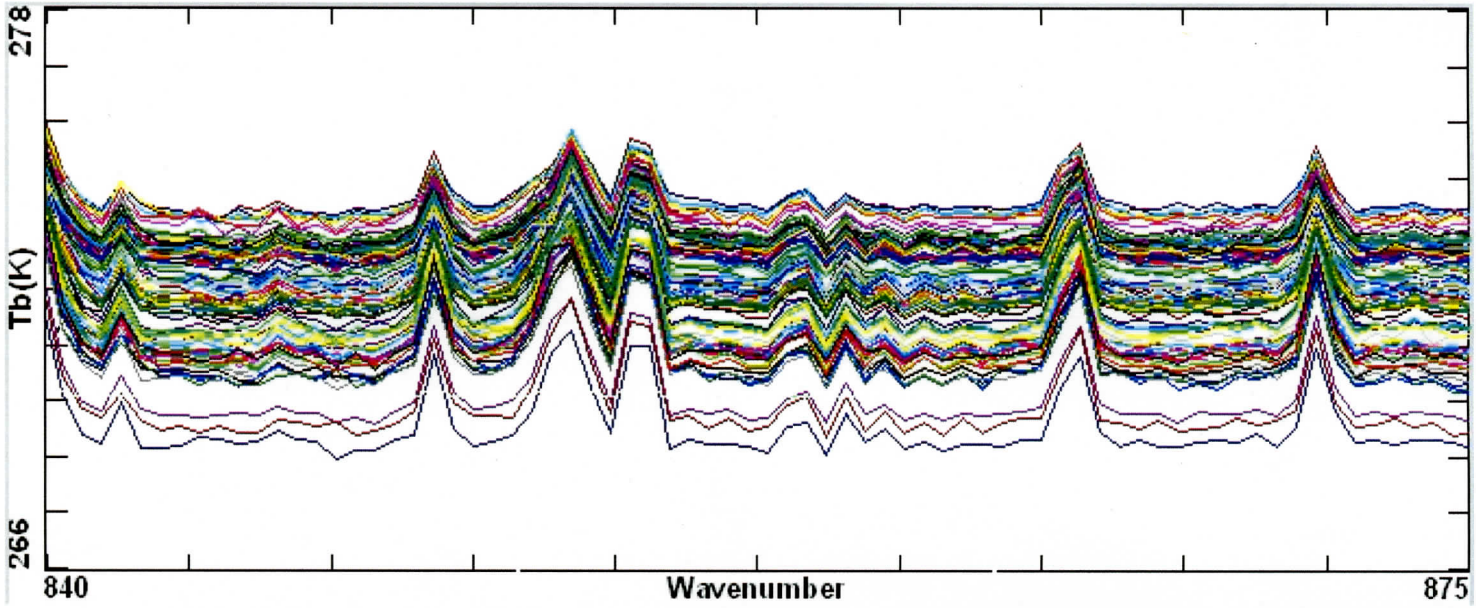

Unfiltered

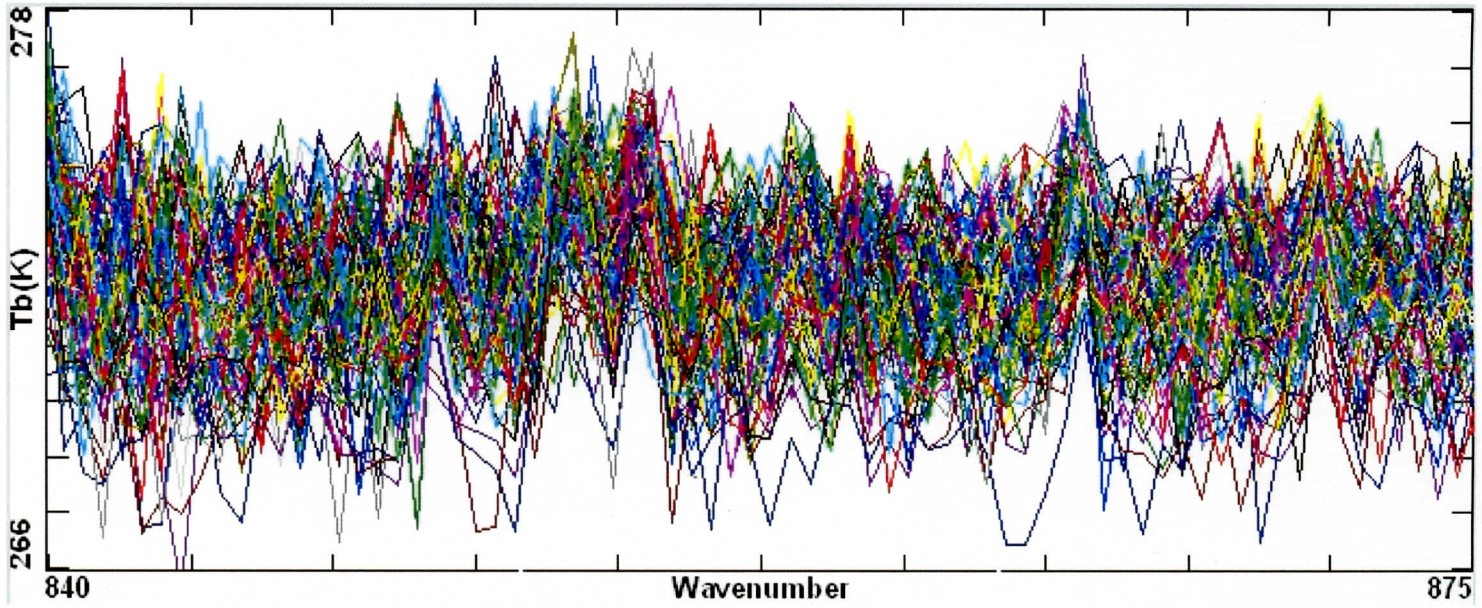

100 Single S-HIS SW Radiance Spectra

Random Noise-Filtered and Unfiltered (Rec 4001-4100)

Filtered

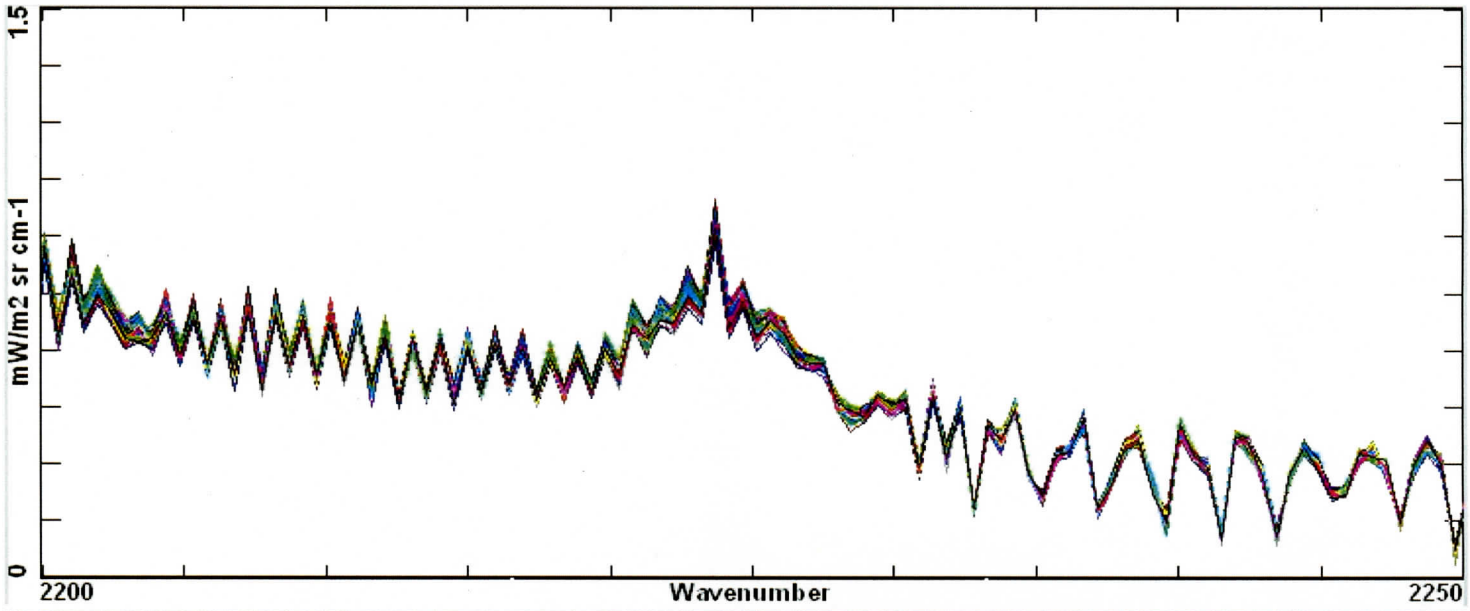

Unfiltered

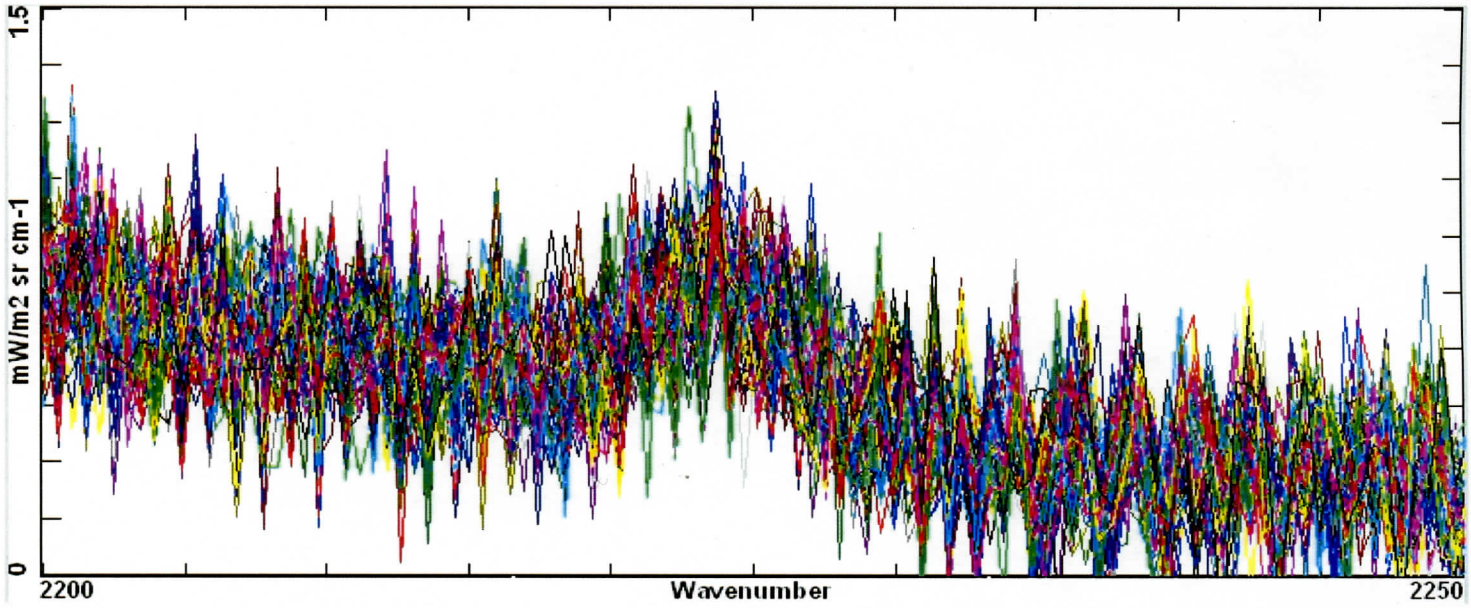

12-10-00 AFWEX

Summary

- Scanning HIS and NAST are providing invaluable experience with high spectral resolution observations in preparation for CrIS (and AIRS)
- Tilt monitoring & tilt-noise correction procedures are being demonstrated on Scanning HIS
- CrIS Applicability of lessons learned on tilt-noise should be evaluated as soon as possible
- PCA Random Noise Filtering potential is only recently being recognized for many applications